NASA TECHNICAL NOTE

NASA TN D-4325

C. 1

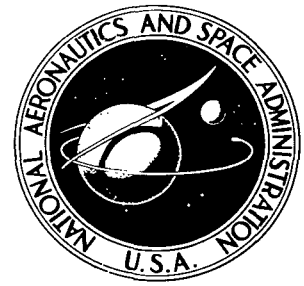

NASA TN D-4325

RESULTS OF INCLUDING A BOUNDARY SHOCK WAVE IN THE CALCULATION OF THE FLIGHT PARAMETERS OF A LARGE HIGH-SPEED METEOR

by E. Dale Martin

Ames Research Center
Moffett Field, Calif.

NATIONAL AERONAUTICS AND SPACE ADMINISTRATION • WASHINGTON, D. C. • MARCH 1968

RESULTS OF INCLUDING A BOUNDARY SHOCK WAVE IN THE CALCULATION OF THE FLIGHT PARAMETERS OF A LARGE HIGH-SPEED METEOR

By E. Dale Martin

Ames Research Center
Moffett Field, Calif.

NATIONAL AERONAUTICS AND SPACE ADMINISTRATION

For sale by the Clearinghouse for Federal Scientific and Technical Information
Springfield, Virginia 22151 – CFSTI price $3.00

TABLE OF CONTENTS

	Page
SUMMARY	1
INTRODUCTION	2
THE NATURE OF, AND CONDITIONS FOR OCCURENCE OF, A BOUNDARY SHOCK WAVE IN RAPID VAPORIZATION	3
ANALYSIS	5
General	5
Shape Factor	11
Conservation Equations for Meteor Motion and Heating	13
Equations for Ablation Process and Boundary Shock Wave	15
Construction of Data Curve	17
Calculation of Flight Parameters	19
RESULTS AND DISCUSSION	21
CONCLUDING REMARKS	25
APPENDIX A - PRINCIPAL NOTATION	28
APPENDIX B - DERIVATION OF THE ONE-DIMENSIONAL CONSERVATION EQUATIONS	32
APPENDIX C - ADDITIONAL RESULTS FROM CONSERVATION EQUATIONS	41
APPENDIX D - CALCULATION PROCEDURE	45
APPENDIX E - ESTIMATION OF THE VAPOR-ABLATION REYNOLDS NUMBER	48
REFERENCES	51
TABLES	53

RESULTS OF INCLUDING A BOUNDARY SHOCK WAVE IN THE CALCULATION OF THE FLIGHT PARAMETERS OF A LARGE HIGH-SPEED METEOR

By E. Dale Martin

Ames Research Center

SUMMARY

The results of including a boundary shock wave in the calculation of the flight parameters of a large high-speed meteor with rapid vapor ablation are investigated. The boundary shock wave, a thin viscous region in a gas flowing rapidly (at high Reynolds number) out of a surface, is characterized by heat conduction and viscous-compressive stresses such as occur in a shock wave. The viscous effects represent the translational nonequilibrium induced in the extreme cases of very rapid vaporization produced by absorption of intense heat radiation at the surface.

Calculations for the particular case of the Ondřejov meteor Příbram use a data curve fitted graphically to the meteor-tracking data. These calculations, based on the approximate tracking data and on gross approximate equations describing the vaporization process, indicate that the proper range of conditions was present on the Příbram meteor, for a significant portion of its trajectory, for a very thin, strong boundary shock to occur at the meteor surface in the vapor, according to the boundary-shock-wave theory. The ablation Reynolds number was high, and significant ratios of density and pressure across the boundary shock wave result from the calculations. The meteor entered the atmosphere at about 20.9 km/sec. At an altitude of 55 km, where the meteor radius was indicated in the idealized calculation to be 18.6 cm, the order of magnitude of the calculated boundary-shock thickness was in the order of 1/1000 times the entire thickness of the vapor layer, or about 7×10^{-4} cm. Although the usual convective heat transfer from the hot air layer was completely blocked by the efflux of vapor, an estimate according to this theory indicates high heat conduction at the surface in the boundary shock (at least 20 percent as large as the radiative heating).

Accounting for the effects of the boundary shock wave substantially decreases the pressure drag, but the viscous-compressive drag is high, so the effective drag coefficient (at least in this simplified analysis) is virtually unchanged by the presence of the boundary shock. Although heat conduction in the boundary shock is high, it is balanced by the work of blowing off the vapor against the resistive force due to the viscous stress, and the overall heating of the body is little affected.

Detailed calculations of the flow about a large high-speed meteor would be significantly influenced by the boundary-shock effects, but overall gross

values of the heating and motion parameters calculated by methods used recently by H. J. Allen and N. A. James are valid because of their use of appropriate assumed values of certain parameters.

INTRODUCTION

An investigation is undertaken to determine what possible effects a boundary shock wave may have in a simplified calculation of the flight parameters of a large high-speed meteor and to determine qualitatively the significance of including consideration of the boundary shock wave in this calculation. A recent theoretical study (ref. 1) investigated the possible occurrence of the boundary shock wave, a thin region where viscous-flow effects predominate in the rapidly ablating vapor very near the molten surface of a body, such as a meteor under certain conditions, moving at a very high speed through the atmosphere. The viscous effects in the vapor are effects of the translational nonequilibrium induced by the very high rate of vaporization with its attendant high rate of heat conduction into the body.[1] In the thin viscous region at the body surface in the vapor, viscous-compressive stresses (as in a shock wave), accompanied by heat conduction, would be present, in contrast to the viscous shearing stresses present in boundary-layer-type flows. However, the layer is much like a boundary layer in that it is adjacent to a wall and has inviscid flow on only one side. The thickness of the viscous region becomes vanishingly small as the Reynolds number of the efflux becomes large, as is true for either a shock wave or a boundary layer when the appropriate Reynolds number is large.

The rapid change of the flow variables across a boundary shock wave could significantly affect the flow pattern of the vapor in front of the meteor. One would then be interested in whether the viscous effects, if they occur, might also influence significantly the motion and heating of the meteor. The purpose here, then, is to investigate a known physical situation having conditions under which the boundary shock wave would be possible (according to the theory of ref. 1) in order to determine the effects.

The importance to aerodynamicists, who are concerned with hypervelocity continuum flow, of acquiring and being able to understand and interpret the data from flight observations of meteors has been discussed recently by Allen (ref. 2) and Allen and James (ref. 3). Before knowledge of meteor phenomena can be applied to the technology of high-speed missiles and space vehicles, aerodynamicists must have sufficient understanding to predict at least approximately the motion and heating of meteoric bodies with known characteristics. Recent analytical studies (see ref. 3) have been very successful in this respect.

In the analysis presented here, attention will be confined to stone meteors with vapor ablation rapid enough that the vapor flow divides into

[1]A more detailed description of boundary shock waves is contained in the section immediately following the Introduction.

inviscid and thin viscous regions (see Analysis). Of particular interest is the Ondřejov meteor Příbram, a stone meteorite that fell in Czechoslovakia in 1959, for which tracking data were obtained by the Ondřejov Observatory (ref. 4) and for which the mass density is known from recovered fragments. The Příbram meteor undoubtedly had a high rate of vapor ablation over most of the portion of the trajectory for which the data were taken, so it is a good example for the study of the boundary-shock effects.

Many idealizations are made in the analysis because of unknown physical properties, but the order-of-magnitude results obtained are expected to be qualitatively useful. Precise calculation of the motion and heating of a large high-speed meteor to determine the effects of a boundary shock wave would require detailed analysis of the flow field surrounding the meteor. However, it was deemed appropriate to approach the calculation here in much the same manner as in reference 3. Rather than a detailed flow-field analysis, then, this study uses the meteor-tracking data for velocity and acceleration, which are carefully fitted graphically to what is believed to be the most reasonable form for the data curve. For the calculation, a set of equations to determine the appropriate meteor parameters is formulated, which includes use of: (1) the previously derived results of reference 1 for the equations relating conditions across the boundary shock wave, (2) conservation equations and other relations incorporating certain appropriate assumptions about the flow around the meteor, and (3) points from the curve fitted to the meteor-tracking data as input. The approximate analysis assumes one-dimensional flow of the ablating vapor and constant average values of flow variables over the meteor face and employs a shape factor to account for either a sphere or a flat-face body. For gross results, such an approach is customary (ref. 3) except that the shape factor was not needed before (see below). More complete conservation equations than have been used previously are derived. These equations and the derivation contain useful information not obtainable from less complete statements of the conservation principles.

THE NATURE OF, AND CONDITIONS FOR OCCURRENCE OF, A BOUNDARY SHOCK WAVE IN RAPID VAPORIZATION

A boundary shock wave is most easily understood as a region of translational nonequilibrium in a molecular flow at a very high rate out of a surface. (Adequate understanding of it therefore requires some background in the basic concepts of modern kinetic theory, for which the reader is referred, e.g., to refs. 5-7.)

Translational nonequilbrium in a molecular flow is manifested macroscopically by the "transport processes" of viscosity and heat conduction. Translational nonequilibrium is also induced by application of significant viscous stress or heat conduction in, or at the boundaries of, any region of gas flow. (The familiar fluid-dynamic boundary layer is a region of translational nonequilibrium induced by shear at a wall; the familiar gas-dynamic shock wave can be thought of as a region of translational nonequilibrium induced by the diffusion or mixing, and subsequent rapid accommodation, of the molecules of one equilibrium average state into a different equilibrium

average state, which necessarily entails heat conduction.) Sufficiently far from any source of translational nonequilibrium, the gas flow relaxes to a local-equilibrium state (or decays to an "inviscid flow"). "Sufficiently far from any source . . ." is equivalent to saying "for a sufficiently large Reynolds number based on distance from the source" or to "for a sufficiently large distance for diffusion of the transport phenomena" (cf. ref. 8, especially pp. 21-23).

During vaporization at a very high rate, produced by absorption of intense heat radiation and subsequent heat conduction back toward the liquid in the vaporization region, it is expected that as the vaporization proceeds to a sufficiently high rate, the associated heat conduction will become strong enough to induce significant translational nonequilibrium in the vapor as it leaves the molten surface. The translational nonequilibrium is induced because of the lag in transferring energy from the molecular translational degree of freedom normal to the surface to the lateral degrees of freedom of the molecules. The lag occurs because of the spaces between the molecules as they are separating in the phase-change region. From kinetic theory, this lag, or difference, in the distribution of molecular energy in one direction from that in another direction is understood as the essence of translational nonequilibrium, including viscosity and heat conduction. This translational nonequilibrium (viscosity and heat conduction) then requires a certain number of collisions, and hence a certain time and distance of flow from the wall, to "equilibrate," or to relax to a condition of flow in local translational equilibrium (inviscid flow). The relaxation distance is the thickness of the boundary shock wave.

From the Chapman-Enskog procedure of kinetic theory, it is found that a gas flow in local translational equilibrium is governed by the Euler equations of inviscid flow and that regions of flow not too far from local translational equilibrium are adequately described by the Navier-Stokes equations of viscous flow. It is known (e.g., ref. 9) that the structure of a sufficiently weak shock wave (and of a downstream portion of a strong shock wave) is accurately described by a solution of the Navier-Stokes equations.

In a boundary shock wave the viscous stress is compressive (rather than shearing) as in a normal shock wave; and also, as in a shock wave, the viscous dissipation is accompanied by heat conduction back through the gas flow. The same equations govern the flow through a plane boundary shock (or through a very thin curved boundary shock) as govern the flow through a shock wave. Reference 1 used the Navier-Stokes formulation to obtain the conditions across a boundary shock, which are represented by equations given below in the subsection "Equations for Ablation Process and Boundary Shock Wave." In a private communication, Prof. H. Schlichting has referred to the solution for the boundary shock wave given in reference 1 as "a . . . generalization of the known solution for the normal shock wave." It is a generalization in the sense that a boundary at upstream infinity can be brought into the region of the rapid transition; or alternatively, the limiting, or degenerate, case of a boundary shock wave as the boundary moves upstream to infinity relative to the rapid-transition region, or equivalently as the boundary shock "detaches" from the wall (as the heat conduction vanishes in a supersonic efflux), is a simple shock wave. From another point of view, a wall can simply be inserted

at any point in a simple shock-structure solution; the values of the various flow quantities at that point are then the boundary conditions, and the downstream portion of the original shock structure then represents the structure of a possible boundary shock wave.

In reference 10, the necessary and sufficient conditions for a boundary shock wave to occur were shown to be

(a) large Reynolds number based on conditions at the boundary of the vapor, and

(b) significant heat conduction or viscous stress (significant translational nonequilibrium) at the boundary.

More thorough discussion of boundary shock waves and the development of the theory is contained in reference 10, including description of the asymptotic treatment of the translational nonequilibrium flow, with emphasis on the boundary conditions, and including discussion of the appropriateness of the equations used in the approximate treatment of the phase change.

ANALYSIS

General

A large meteoric body of the type that would experience a high rate of vapor ablation while moving at very high speed through the earth's atmosphere is shown in sketch (a).[2] If the observer were moving with the meteor, one would expect the instantaneous flow pattern to be qualitatively as shown in the sketch. (The curved lines, except the one indicated as the shock wave, are streamlines.) The very high rate of vapor ablation is to be expected for a large high-speed stone meteor such as the Ondřejov meteor Příbram (see ref. 3).

[2]The meteoric body sketched is nearly spherical. Very large, very high-speed meteors would be expected to have a nearly spherical shape because of their high rates of ablation and their general rotational motion. Virtually no spherical meteorites are found, however, for the following reasons: Meteoric bodies that are either too small or too slow will not have experienced the extreme ablation and hence will, in general, be irregular in shape (see ref. 11). Nearly all (if not all) the fireballs that reach the earth without vaporizing completely will have fragmented at some point of the trajectory (ref. 11) and hence will also be irregular.

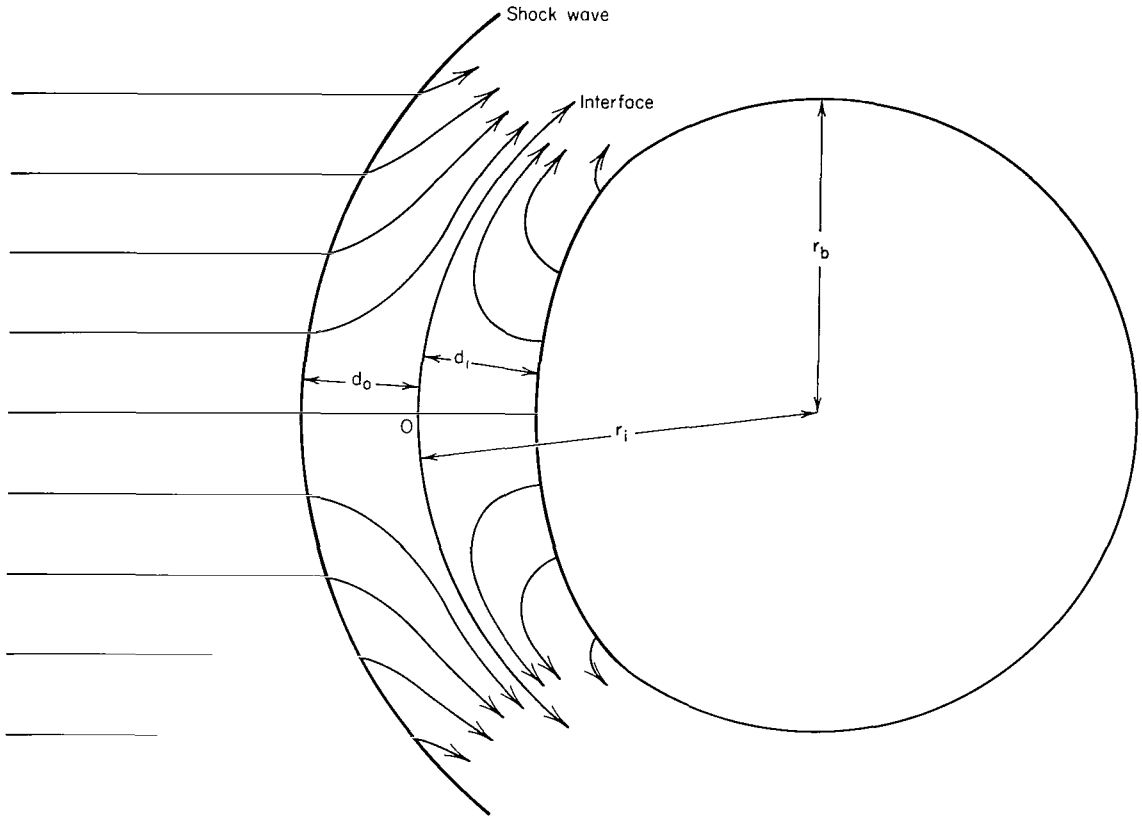

Sketch (a).- Flow configuration.

Although a detailed flow-field analysis is not made here, it is important to understand the qualitative structure of the flow. The following characteristics of the structure should be noted (refer to both sketches (a) and (b)): A stagnation point exists at point O, on the interface between the hot compressed air and the vapor ablating from the meteor face. For large Reynolds number $\rho_2 u_2 d_O/\mu_2$ (notation is defined in appendix A), the flow of hot compressed air around the meteor is essentially inviscid except for the very thin shock wave and a thin layer at the interface. For large Reynolds number, $\rho_b u_b d_i/\mu_b$, the flow of meteoric vapor is also essentially inviscid except for the thin viscous region at the interface and the thin boundary-shock region (see ref. 1). The three viscous regions - the shock wave, the interfacial layer, and the boundary shock wave - may be treated as surfaces of discontinuity of certain variables in the inviscid flow. It can be shown that only the pressure is required to be continuous across the interface (in the inviscid limit). Hence, the pressure p_O is the stagnation pressure on the axial streamline between point 2 and point e in sketch (b).

The high temperature air in the outer shock layer radiates heat to the meteor surface at a high rate. The large energy flux to the surface produces

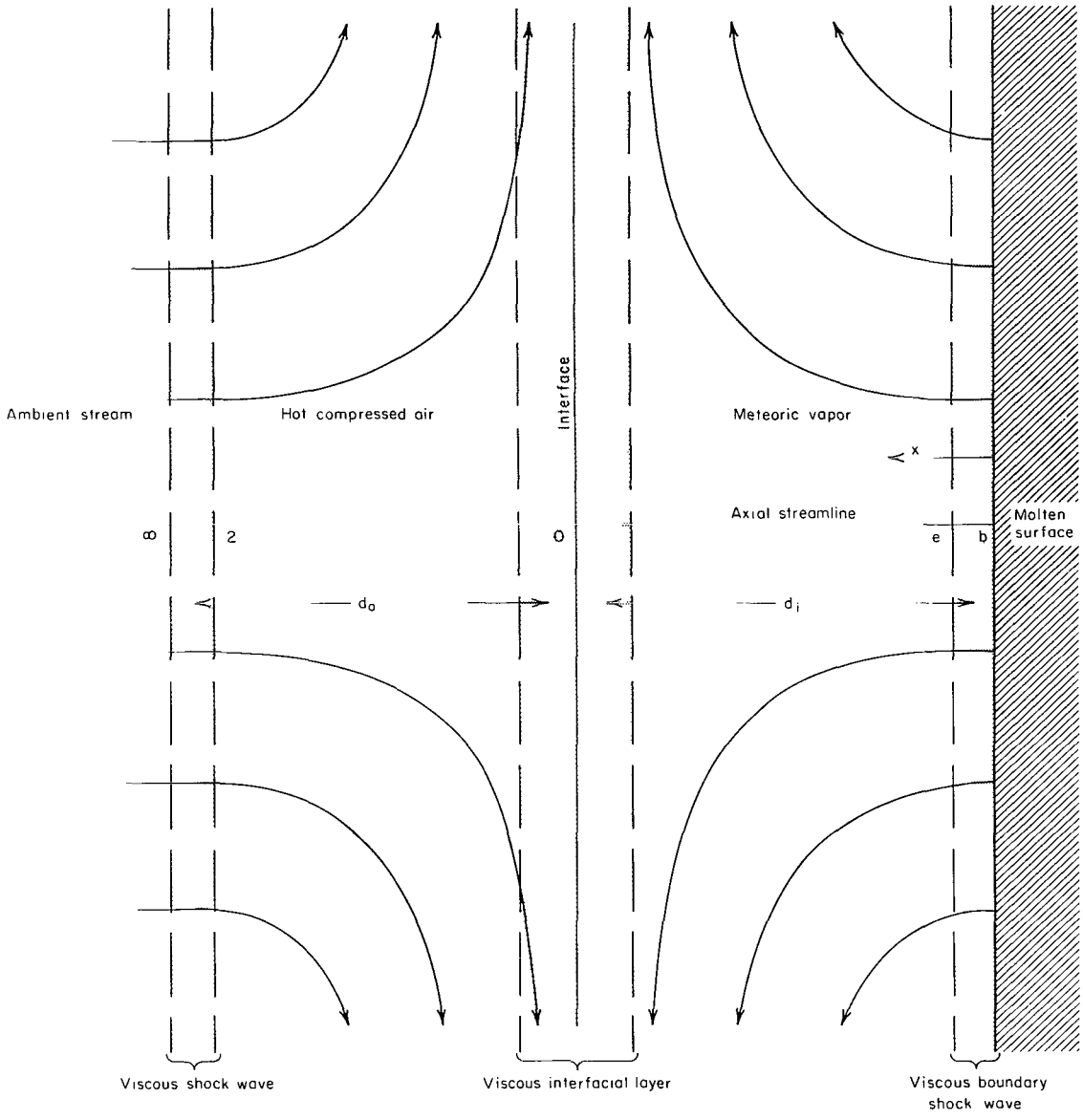

Sketch (b).- Viscous and inviscid regions in flow near body axis.

the high rate of vapor ablation.[3] The hot air and vapor are arbitrarily assumed to be transparent to radiation, and the radiation is assumed to be

[3]For small or relatively slow meteors, heating by friction with the air (convective heating) produces ablation of the meteor surface. In the case of the fireball, at least in the major portion of the trajectory where the heating is most intense, the meteor is being heated not by friction with the air but by heat radiation from the highly compressed air behind the shock wave. Heating by friction, or convective heat transfer to the body, is almost nonexistent in this case, as will be seen later. However, an additional source of heat conduction is considered here: the viscous dissipation associated with the translational nonequilibrium in the thin region adjacent to the liquid layer.

absorbed within a very short distance inside the liquid surface. Radiation absorption by the vapor may be important. However,

(a) The radiation properties of the vapor are unknown; therefore, some assumption must be made in order to study the qualitative features of the flow;

(b) Neglect of the absorption by the vapor simply changes the magnitude of the radiation absorbed at the liquid surface, which should not alter the qualitative results unless the amount of radiation received by the body is changed by orders of magnitude;

(c) The vapor is at a much lower temperature than the hot air in the outer layer, which tends to decrease the importance of absorption by the vapor.

Since the meteoric-stone material has low thermal conductivity, only the surface is at the vaporization temperature; it is assumed that vapor forms only at the surface, and little or no bubble formation is expected to accompany the "boiling off" of the vapor. In addition, the high viscosity of the molten meteoric stone prevents the spraying of liquid drops along with the efflux of vapor (ref. 12).

Allen (ref. 3) has pointed out that meteors of the type considered here tend to be spherical, but may be somewhat flattened by ablation due to large rates of radiative heating (see sketch (a)). Moreover, the present desire is to obtain only gross effects; we therefore take advantage of the great simplification provided in the analysis by roughly approximating the flow as being one-dimensional near the meteor surface. That is, we take constant values for the variables over the meteor face and consider the area of the meteor face to be equal to the cross-sectional area, πr_b^2, for the purpose of computing drag and heat transfer to the body. The flatter the face, the more nearly constant are the variables, so the results would be most applicable to a flat-face body of area πr_b^2. The application to a spherical body may be made in an approximate way by introducing a shape factor, as described in the next section. The one-dimensional approach described above is equivalent to the approach used by Allen and James (ref. 3), who obtained consistently good results in general. However, Allen and James did not need to use the shape factor for the sphere, since they assumed an effective drag coefficient equal to unity, which is appropriate to a sphere, so that a shape factor was effectively "built in." In the present analysis, the drag coefficient will be calculated rather than assumed, so, as will be seen, the shape factor is needed here and its use yields consistent results.

With this background, a procedure can now be formulated to calculate approximately the effects of the boundary shock wave on the meteor flight parameters. The altitude-density function, $\bar{\rho}$, of reference 3 (see also table I) will be used, where

$$\rho_\infty = \rho_{SL}\bar{\rho} \tag{1}$$

is the ambient density at altitude h and

$$\rho_{SL} = 1.225 \times 10^{-3} \text{ gm/cm}^3 \tag{2}$$

is the ARDC standard atmosphere density at sea level (ref. 13). The density ratio across a normal shock wave (needed in the calculations that follow) is approximately equal to the ratio of the ambient-stream density to the stagnation density behind the shock and, hence, is given for $V > 7.5 \times 10^5$ cm/sec by the approximate relation (cf. ref. 14, p. 50)

$$\tilde{k} \equiv \frac{\rho_\infty}{\rho_2} = \frac{\bar{\rho}^{0.039} \left(\dfrac{V}{10^2 \text{ cm/sec}} \right)^{0.16}}{54.5} \tag{3}$$

To compute the heat radiation incident on the meteor face, one needs to know the volume of the outer shock layer. For a spherical nose at high hypersonic Mach number, the ratio of the shock standoff distance to the sphere radius is given approximately by Lighthill's solution (ref. 15). In the present case, the air-vapor interface would be the equivalent body, so that, assuming the interface to be nearly spherical (see sketch (a)), one can approximate the outer standoff distance d_o by a form equivalent to Lighthill's solution. Using the definition

$$\frac{d_o}{r_i} \equiv \bar{D} - 1 \tag{4}$$

where

$$r_i \approx r_b \tag{5}$$

one can obtain $\bar{D}$ implicitly as the appropriate root of

$$\lambda \equiv 3(1 - \tilde{k})^2 + 5(4\tilde{k} - 1)\bar{D}^2 + 2(1 - \tilde{k})(1 - 6\tilde{k})\bar{D}^5 = 0 \tag{6}$$

For the radiation rate per unit volume of the outer shock layer, which we denote as I, the relation given in reference 14, approximately valid for $V > 13.7 \times 10^5$ cm/sec, is

$$\left(\frac{I}{1 \text{ erg cm}^{-3} \text{ sec}^{-1}} \right) = 6.44 \times 10^{-5} \, \bar{\rho}^{1.8} \left(\frac{V}{10^2 \text{ cm/sec}} \right)^{5.05} \tag{7}$$

(Results obtained from use of this equation should be considered in the light of the qualifications made by the authors of reference 14.) In view of the discussion above, and with the assumption that one-half the radiation emitted by the outer shock layer impinges on the body, we represent the total radiative heating rate to a spherical body with a flattened face as

$$Q_r = \frac{1}{2} \pi r_b^2 I d_o \tag{8}$$

and define the radiative-heat-transfer coefficient[4] as

$$(C_{H_r})_{ff} \equiv \frac{Q_r}{\frac{1}{2}\rho_\infty V^3(\pi r_b^2)} = \frac{Id_o}{\rho_\infty V^3} \tag{9}$$

Since d_o/r_b is known from equations (4), (5), and (6), the value of $(C_{H_r}/r_b)_{ff}$ at any altitude for a flat-face body is found from

$$\left(\frac{C_{H_r}}{r_b}\right)_{ff} = \frac{I}{\rho_\infty V^3}\left(\frac{d_o}{r_b}\right) = \frac{I}{\rho_\infty V^3}(\bar{D} - 1) \tag{10}$$

where V is to be obtained from the meteor data.

The effect of the forces (other than body forces) that produce the changes in motion of the meteor may be represented parametrically by an effective drag coefficient (cf. ref. 3), defined by the relation

$$\left.\begin{aligned} C_{D_{eff}} \frac{1}{2}\rho_\infty V^2(\pi r_b^2) &= m\left(-\frac{dV}{dt} + \tilde{f}\right) \\ &= m\left(-\frac{dV}{dt} + g \sin\theta\right) \end{aligned}\right\} \tag{11}$$

where the meteor mass m is approximately

$$m = \frac{4}{3}\pi r_b^3 \rho_m \tag{12}$$

and ρ_m is the mass density of the meteor. (See table II for the physical constants needed in this and other sections below. The value $\rho_m = 3.5$ gm/cm^3 corresponds to the Ondřejov meteor Příbram (ref. 3) and is also nearly equal to the value 3.4 used by Öpik (ref. 12) for typical stone meteors.) From equations (11) and (12), $C_{D_{eff}}/r_b$ is known:

$$\frac{C_{D_{eff}}}{r_b} = \frac{8}{3}\frac{\rho_m}{\rho_\infty V^2}\left(-\frac{dV}{dt} + g \sin\theta\right) \tag{13}$$

In the calculation it is convenient to use the quantity

$$Z \equiv \frac{VC_{H_r}}{C_{D_{eff}}} = \frac{V\left(\frac{C_{H_r}}{r_b}\right)}{\frac{C_{D_{eff}}}{r_b}} \tag{14}$$

[4]The reflectivity of the vaporizing surface material was disregarded because it is not known.

where C_{H_r}, for a body that does not have a flat face, is related to $(C_{H_r})_{ff}$. That relationship will be considered later. An expression for p_e, the pressure outside the boundary shock wave, will also be needed. Note first that the pressure at the stagnation point 0 is the stagnation pressure along the line 2-0-e in sketch (b) and is given approximately by

$$p_o = \rho_\infty V^2 \tag{15}$$

Then the ratio of the pressure p_e to the stagnation pressure is given in terms of the Mach number outside the boundary shock wave, M_e, and the ratio of specific heats in the vapor, γ (assumed constant), as (e.g., cf. ref. 16, p. 53)

$$\frac{p_e}{p_o} = \left(1 + \frac{\gamma - 1}{2} M_e^2\right)^{\frac{-\gamma}{\gamma - 1}} \tag{16}$$

Based on the general ideas and formulations developed in this section, the equations needed to determine the flight parameters will be presented in the following sections, which include a summary of the calculation procedure.

Shape Factor

If the one-dimensional analysis with constant variables on the meteor face is used for flow near the meteor surface, the resulting equations are most appropriate to a flat-face body unless an assumed value of $C_{D_{eff}}$ appropriate to a sphere is used, as done by Allen and James in reference 3. When the value of $C_{D_{eff}}$ is not assumed, an appropriate shape factor must be used, if the equations are to be applied to a nearly spherical body, to insure realistic results.

To derive a reasonably realistic shape factor, consider the following: Suppose a sphere and a flat-face body have the same cross-sectional area, πr^2, and that some variable ψ on the surface has a constant value ψ_o on the flat face normal to the flow and varies as

$$\psi = \psi_o \cos^n \varphi \tag{17}$$

over the front half of the sphere, where φ is the angle between the axis, or stream direction, and a radial line of the sphere through a point on the surface. Let Ψ be the integrated value of ψ over the front surface area. Then, for the flat face,

$$\Psi_{ff} = \pi r^2 \psi_o \tag{18}$$

and, for the sphere,

$$\left.\begin{aligned} \Psi_{\text{sphere}} &= \int_S \psi \, dS = \int_0^{\pi/2} \psi_o \cos^n \varphi (2\pi r^2 \sin \varphi \, d\varphi) \\ &= \pi r^2 \psi_o \int_0^{\pi/2} 2 \cos^n \varphi \sin \varphi \, d\varphi \\ &= \frac{2}{n+1} \Psi_{ff} \end{aligned}\right\} \tag{19}$$

Suppose now one wants to compute the total radiative heat transfer to the surface for a heat flux that varies approximately as $\psi_o \cos^n \varphi$. The radiative-heat-transfer coefficients would then be related by

$$(C_{H_r})_{\text{sphere}} = \frac{2}{n+1} (C_{H_r})_{ff} \tag{20a}$$

where $(C_{H_r})_{ff}$ is given by equation (9) or (10). Now let the radiative-heat-transfer coefficient to be calculated for the meteoric body be represented by

$$C_{H_r} = \frac{1}{s_H} (C_{H_r})_{ff} \tag{20b}$$

where s_H is a shape factor for heat transfer. If, for example, the body is a sphere and if the radiative heating rate varies as $\cos^3 \varphi$, for which $n = 3$ in equation (20a) (cf. fig. 9 of ref. 17), then $s_H = 2$. Thus,

$$\left.\begin{aligned} &s_H = 2 \text{ for sphere with } q_r/q_{ro} = \cos^3 \varphi \\ &s_H = 1 \text{ for flat-face body} \end{aligned}\right\} \tag{21a}$$

Similarly, suppose one wants to compute drag due to a force per unit area normal to the surface that varies approximately as $\psi_o \cos^2 \varphi$ (a reasonable assumption; true for Newtonian flow). Then the force per unit area parallel to the axis would be $\psi = \psi_o \cos^3 \varphi$. Using equation (19), one then finds the drag of a sphere to be one-half the value on the flat face (since $n = 3$). Thus, assume

$$C_{D_{eff}} = \frac{1}{s_D} (C_{D_{eff}})_{ff} \tag{22}$$

where the shape factor for drag, s_D, is

$$\left.\begin{aligned} &s_D = 2 \text{ for sphere} \\ &s_D = 1 \text{ for flat-face body} \end{aligned}\right\} \tag{21b}$$

Further, for convenience and in view of equations (21a) and (21b), consider a common shape factor for heat transfer and drag:

$$s = s_H = s_D \tag{21c}$$

An appropriate value for s may be determined as that value which causes $C_{D_{eff}}$ to be unity at high altitude. For the Příbram meteor,

$$s = 2 \tag{21d}$$

gives this result.

The quantity Z in equation (14) is now

$$Z \equiv \frac{VC_{H_r}}{C_{D_{eff}}} = \frac{\frac{1}{s} V \left(\frac{C_{H_r}}{r_b}\right)_{ff}}{\frac{C_{D_{eff}}}{r_b}} \tag{14'}$$

Conservation Equations for Meteor Motion and Heating

Now consider an equivalent flat-face body with uniform values of flow parameters over the meteor face, for which we want to write one-dimensional flow conservation equations. The one-dimensional equations of conservation of mass, momentum, and energy of the meteoric body can be developed in several ways. One derivation is given in appendix B for conditions and assumptions corresponding to the description in the above section. In appendix B the conservation principles are combined into equations (B8a) and (B28) which may be designated, respectively, as the momentum equation and the energy equation. These may be written, neglecting ρ_b/ρ_s in comparison to unity, as

$$\left[\frac{m}{A}\left(-\frac{dV}{dt} + \tilde{f}\right)\right]_{ff} = \rho_b u_b^2 + p_b - \tau_b \tag{23}$$

$$-(q_r + q_{c_b})_{ff} = \rho_b u_b \left(\zeta_{ab} + \frac{1}{2} u_b^2\right) - \tau_b u_b \tag{24}$$

where ζ_{ab} is given by equation (B16) as

$$\zeta_{ab} = c_{sol}(T_f - T_a) + L_f + c_{liq}(T_b - T_f) + L_v \tag{25}$$

where T_a is the cold interior temperature of the meteor. The cross-sectional area A in equation (23) is πr_b^2, in line with the above discussion. The subscript b denotes the value of a quantity in the vapor flow at the boundary, the molten surface of the meteor. The notation is defined in

appendix A, but we point out here for convenience that u_b is the vapor velocity relative to the boundary surface, τ_b the viscous compressive stress at the boundary, and q_{c_b} the associated heat conduction at the boundary (see ref. 1). (Some of the previous equations are discussed in appendix B; further results are discussed in appendix C.)

To put these equations into a form that can be used in the present calculation, we use the definitions (cf. eqs. (9) and (11)):

$$(C_{H_r})_{ff} = \left(\frac{-q_r A}{\frac{1}{2}\rho_\infty V^3 A}\right)_{ff}, \qquad (C_{D_{eff}})_{ff} = \left[\frac{m\left(-\frac{dV}{dt} + \tilde{f}\right)}{\frac{1}{2}\rho_\infty V^2 A}\right]_{ff} \tag{26}$$

It is also convenient to make the approximation

$$q_c = \tau u \tag{27a}$$

and, in particular,

$$q_{c_b} = \tau_b u_b \tag{27b}$$

Equations (27) are exactly true for

$$\widetilde{Pr} \equiv \frac{\tilde{\mu} c_p}{k} \equiv \frac{\left(\frac{4}{3}\mu + \frac{1}{3}\kappa\right) c_p}{k} = 1 \tag{28}$$

and are approximately true in general for $\widetilde{Pr} \neq 1$ (see ref. 1), where μ is the shear-viscosity coefficient, κ the bulk viscosity coefficient, k the coefficient of thermal conductivity in the vapor, and c_p the specific heat at constant pressure in the vapor. Note that if $\widetilde{Pr} = 1$ and $\kappa = 0$, the Prandtl number, $\mu c_p/k$, is then $3/4$. The vapor from a typical stone meteor may be approximated for some purposes as a perfect diatomic gas (see ref. 1), so that, in fact, $Pr \approx 3/4$ and $\widetilde{Pr} \approx 1$ for this case. Equations (23) and (24), substituted into (26) with use of (27b), take the forms:

$$(C_{D_{eff}})_{ff} = \frac{2\rho_b u_b^2}{\rho_\infty V^2}\left(1 + \frac{1}{\gamma M_b^2} + \frac{1}{2} C_{h_c}\right) \tag{29}$$

$$(C_{H_r})_{ff} = \frac{2\rho_b u_b^3}{\rho_\infty V^3}\left(\frac{\zeta_{ab}}{u_b^2} + \frac{1}{2}\right) \tag{30}$$

where

$$C_{h_c} = \frac{-q_{c_b}}{\frac{1}{2}\rho_b u_b^3} = \left(\frac{\rho_\infty V^3}{\rho_b u_b^3}\right)(C_{H_c})_{ff} \tag{31}$$

$$(C_{H_c})_{ff} = \frac{-q_{c_b}}{\frac{1}{2}\rho_\infty V^3} \tag{32}$$

$$M_b^2 = \frac{u_b^2}{\gamma p_b/\rho_b} \tag{33}$$

and γ is the ratio of specific heats in the vapor, c_p/c_v. We may now obtain a second expression for Z (cf. eq. (14)) by dividing VC_{H_r} from equation (30) by $C_{D_{eff}}$ from (29) and (20). For convenience in performing an iterative calculation (to be described later), let us denote this expression by Z' and use equation (33) and the perfect gas equation of state

$$p_b = \rho_b R T_b \tag{34}$$

to eliminate u_b, p_b, and ρ_b. The result is

$$Z' \equiv \frac{VC_{H_r}}{C_{D_{eff}}} = \frac{M_b\sqrt{\gamma R T_b}\left(\frac{\zeta_{ab}}{RT_b} + \frac{1}{2}\gamma M_b^2\right)}{1 + \gamma M_b^2 + \frac{1}{2}\gamma M_b^2 C_{h_c}} \tag{35}$$

which is to be set equal to Z in equation (14') (p. 13) for the final calculation.

Equations for Ablation Process and Boundary Shock Wave

Ablation process.- The temperature T_b at which the vaporization (boiling) takes place depends directly on the pressure to be overcome by the molecules escaping from the liquid (e.g., ref. 18, p. 88) and also on any significant final viscous stress (see appendix B of ref. 1); the mass flux, or the rate of vapor ablation, depends directly on the number of liquid molecules near the surface that have sufficient energy to escape the liquid and on their velocities. The dependence of the temperature of vaporization T_b on the total compressive stress, $p_b - \tau_b$, for the phase transition at constant temperature is taken to be supplied approximately by the modified Clapeyron's equation (appendix B in ref. 1) in the form

$$\frac{p_b - \tau_b}{p_{ref}} = e^{\frac{L_v}{R}\left(\frac{1}{T_{ref}} - \frac{1}{T_b}\right)} \tag{36a}$$

For the model of typical meteoric stone used by Öpik (ref. 12), the mean normal boiling point (boiling temperature at a pressure of 760 mm Hg, or 1.013×10^6 dynes/cm^2) is 2960° K. This can be used as the reference point in equation (36a), so that, using L_v and R from table II, we obtain the following expression for T_b as a function of p_b:

$$\frac{T_b}{1^\circ K} = \frac{36{,}500}{26.13 - \ln\left(\frac{p_b - \tau_b}{1 \text{ dyne/cm}^2}\right)} \tag{36b}$$

The relation used by Öpik (ref. 12, p. 24) to represent the vaporization rate is

$$(\rho u)_b = \frac{1}{2} \rho_b \bar{v}_x \tag{37a}$$

where $(1/2)\bar{v}_x$ is the average molecular-velocity component normal to the surface in the $+x$ direction. For meteoric stone (ref. 12, p. 161), this reduces to

$$\left(\frac{\rho_b u_b}{1 \text{ gm cm}^{-2} \text{ sec}^{-1}}\right) = 3.08 \times 10^{-4} \left(\frac{p_b}{1 \text{ dyne cm}^{-2}}\right) \left(\frac{1^\circ K}{T_b}\right)^{1/2} \tag{37b}$$

which, with use of equation (34), becomes simply

$$M_b = \frac{u_b}{\sqrt{\gamma R T_b}} = \sqrt{\frac{R}{\gamma}} \left(\frac{\rho_b u_b T_b^{1/2}}{p_b}\right)$$

$$= 3.08 \times 10^{-4} \sqrt{\frac{R/\gamma}{1 \text{ cm}^2 \text{ sec}^{-2} (^\circ K)^{-1}}} = 0.333 \tag{38}$$

where the constants from table II have been used.

Boundary shock wave.- At this point we note that, with equations (36b) and (38), Z' in equation (35) is determined in terms of p_b and C_{h_c}, which are still unknown. Since M_b is known and p_e is known in terms of M_e (eq. (16)), it is obvious that equations for the conditions across the boundary shock wave (i.e., conditions relating M_e, p_e, etc., to M_b, p_b, etc.) and for C_{h_c} are needed. If we define the density ratio across the boundary shock wave as

$$\frac{\rho_e}{\rho_b} \equiv \frac{1}{\alpha} \tag{39}$$

we can write the following relationships (developed in ref. 1):

$$\alpha = \frac{M_e}{M_b} \sqrt{\frac{1 + \frac{\gamma - 1}{2} M_b^2}{1 + \frac{\gamma - 1}{2} M_e^2}} \tag{40}$$

$$\frac{T_e}{T_b} = 1 + \frac{\gamma - 1}{2} M_b^2(1 - \alpha^2) \tag{41}$$

$$\frac{p_e}{p_b} = \alpha \frac{M_b^2}{M_e^2} \tag{42}$$

$$C_{h_c} = 2\left[\alpha\left(1 + \frac{1}{\gamma M_e^2}\right) - \left(1 + \frac{1}{\gamma M_b^2}\right)\right] \tag{43}$$

Construction of Data Curve

To use the equations given above for calculating the meteor flight parameters, one needs to know the values for velocity, V, and acceleration, dV/dt, as well as g sin θ, at each altitude, h. One of the most difficult problems of a study such as the present one is how best to use the meteor-tracking data. The data for velocity versus altitude are given in table III (taken from ref. 4, table 7). The data curve (fitted to the data points) must give physically reasonable results. Least-squares fits (see ref. 3) have given realistic results in the past except in the case of Ondřejov meteor Příbram, for which there was some difficulty. The shape of the curve fitted to the data appears to be especially important in the upper part of the trajectory, where the accelerations are small. If one data point is significantly in error or if some supposedly small factor is neglected, the results can be affected significantly.

The view is taken here that the data curve must best fit the tracking data and at the same time yield a physically possible result (in particular, a nonincreasing radius). In constructing the data curves of h versus V, certain appropriate assumptions can be made that allow one to calculate approximately the slopes near the top of the trajectory for different values of an assumed initial radius, r_b*. Then, using these slopes as guides, one can graphically fit a curve to the data. This is, in effect, a combination of fitting a curve graphically to the data and using "approximate isoclines" to determine the shape of a portion of the curve. Of the resulting curves for different r_b*, that value is used for which the results are most consistent along with the best apparent fit to the data.

The procedure for constructing the data curve is as follows: The data, given in table III, are plotted in figures 1(a) through (f). Note from table III that V does not change significantly, especially between, say, h = 90 and 65 km. For this altitude range, assume $V = V^* = 20.87 \times 10^5$ cm/sec. Also assume $C_{D_{eff}}$ does not change much from unity and r_b does not change much from its initial value, r_b*, in this altitude range. These assumptions will be justified by the calculated results. From reference 3, sin $\theta = 0.6853$. From equation (13) we then have the approximate relation for the top part of the trajectory (90 to 65 km altitude):

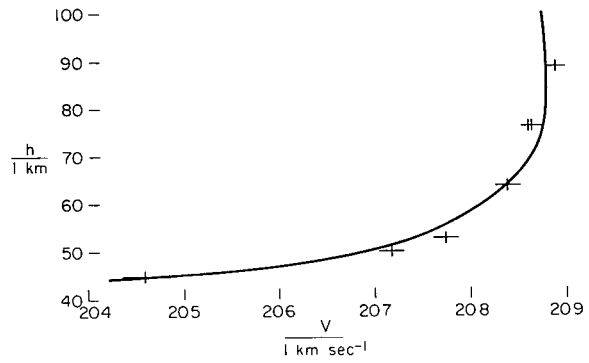

(a) $r_b^* = 10$ cm

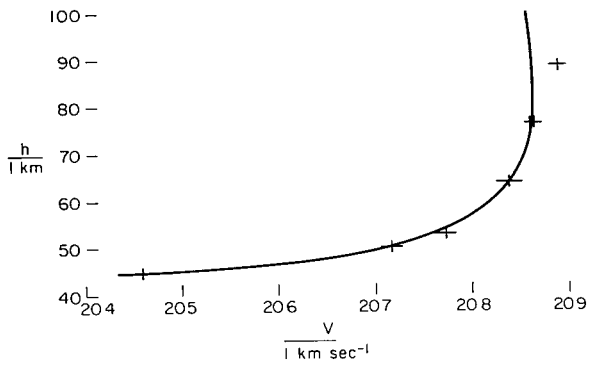

(b) $r_b^* = 15$ cm

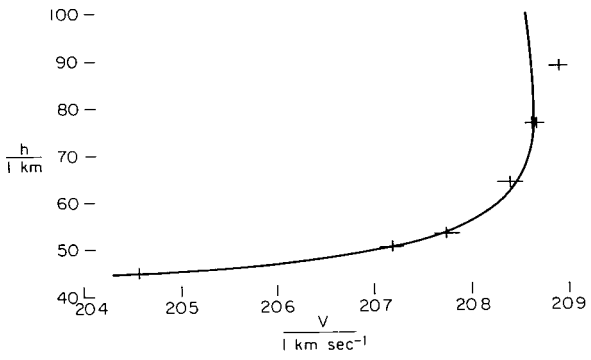

(c) $r_b^* = 20$ cm

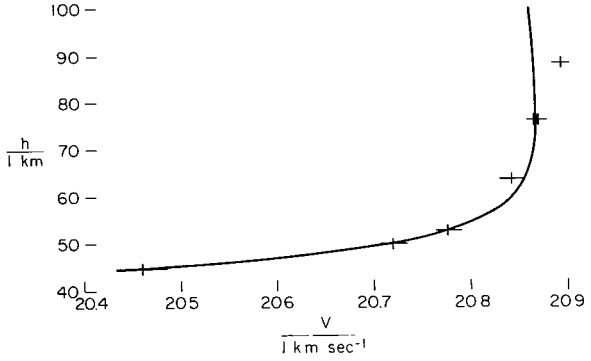

(d) $r_b^* = 25$ cm

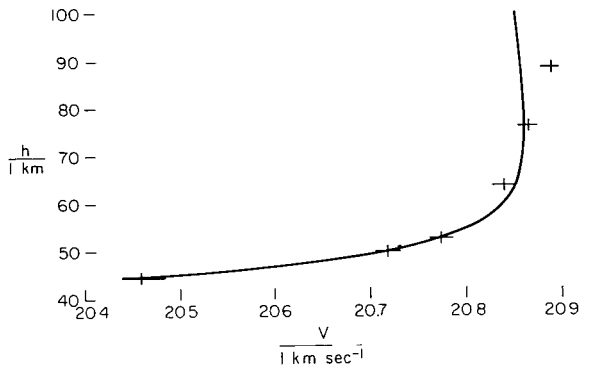

(e) $r_b^* = 35$ cm

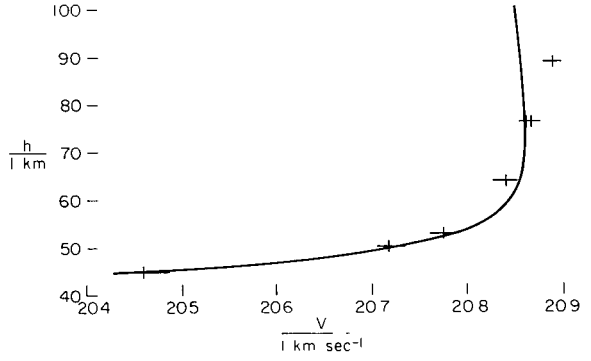

(f) $r_b^* = 50$ cm

Figure 1.- Graphical fit to tracking data of Ondřejov meteor Příbram.

$$\frac{1}{r_b^*} = \frac{8}{3}\frac{\rho_m}{\rho_{SL}}\frac{\left(-\frac{dV}{dt} + g \sin\theta\right)}{\overline{\rho}V^{*2}} \tag{44}$$

Using also

$$\frac{dV}{dt} = -V \sin\theta \frac{dV}{dh} \tag{45}$$

we then obtain for the approximate slope of the h, V curves:

$$\frac{dV}{dh} = \frac{1}{V^*}\left(\frac{3}{8}\frac{\rho_{SL}}{\rho_m}\frac{\overline{\rho}V^{*2}}{r_b^* \sin\theta} - g\right), \qquad \left(65 \leq \frac{h}{1 \text{ km}} \leq 90\right) \tag{46a}$$

or

$$\frac{dV/dh}{1 \text{ sec}} = \frac{399\overline{\rho}}{(r_b^*/1 \text{ cm})} - 4.70\times10^{-4}, \qquad \left(65 \leq \frac{h}{1 \text{ km}} \leq 90\right) \tag{46b}$$

With $\overline{\rho}$ (from table I) and various values of r_b^*, approximate values of dV/dh were calculated from equation (46b) and are listed in table IV. From these values, slopes were drawn on parts (a) through (f) of figure 1. The best curve was drawn through the points guided by these slopes. Since two data points (data from two different cameras) are given for h = 76 km that are very close, those points were assumed to be accurate. On the other hand, the top data point (h = 88 km) was virtually ignored. It was impossible to obtain realistic results using the top data point.[5] The data to be used as input (V and dV/dt) were then obtained from figure 1 for each r_b^* by measuring the slopes and using equation (45). The values are listed in table V.

Calculation of Flight Parameters

For convenience, sketch (c) shows the overall scheme for calculating the flight parameters.

Some parameters of interest that can be calculated, in addition to those already defined, are: the pressure drag coefficient,

$$C_{D_p} = \frac{p_b}{(s/2)\rho_\infty V^2} \tag{47}$$

[5]Note that the data curve of Allen and James (ref. 3 for the same data) also appears to disregard the top point. Note also that the two top data points of table III were obtained with a camera different from that used to obtain the remaining points.

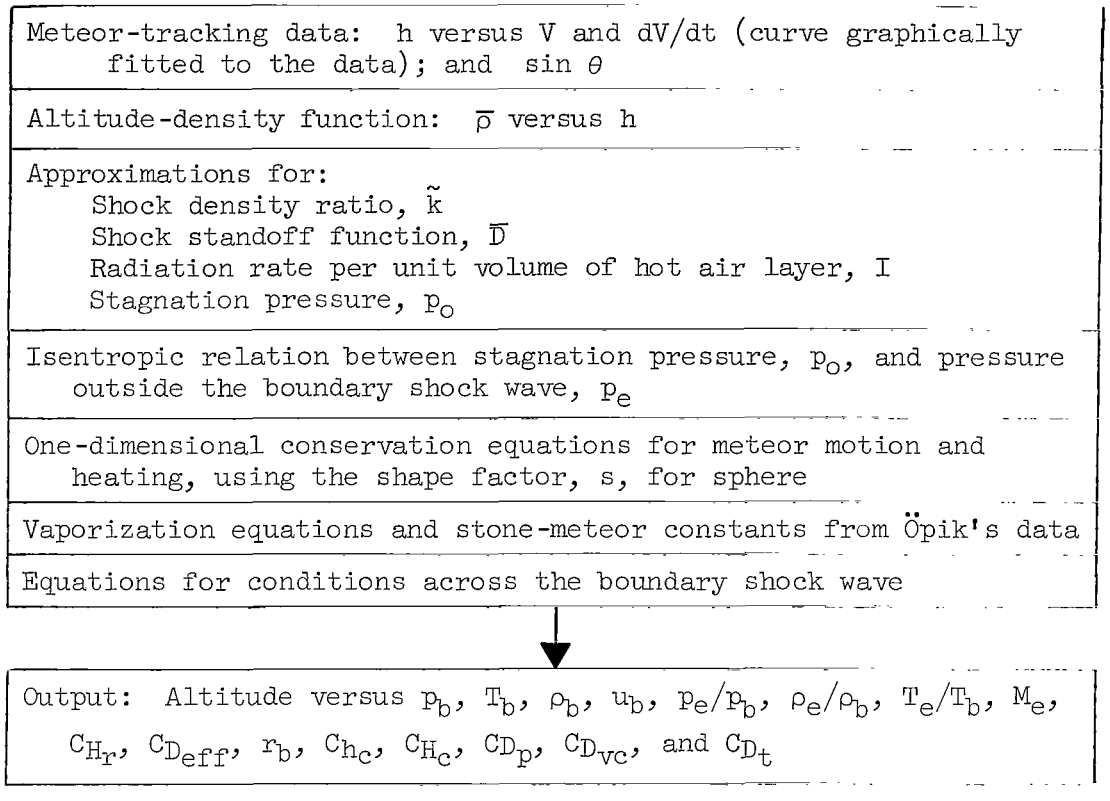

Sketch (c).- Summary of calculation.

the drag coefficient due to the viscous-compressive stress,

$$C_{D_{vc}} \equiv \frac{-\tau_b}{s(1/2)\rho_\infty V^2} = \frac{-q_{c_b}/u_b}{s(1/2)\rho_\infty V^2} = \frac{V}{su_b}\left[\frac{-q_{c_b}}{(1/2)\rho_\infty V^3}\right] = \frac{V(C_{H_c})_{ff}}{su_b} \tag{48}$$

the contribution to the total $C_{D_{eff}}$ due to the retrothrust of the vapor,

$$C_{D_t} \equiv \frac{\rho_b u_b^2}{s(1/2)\rho_\infty V^2} = C_{D_{eff}} - C_{D_p} - C_{D_{vc}} \tag{49}$$

and the heat-transfer coefficients:

$$C_{H_c} = \frac{1}{s}(C_{H_c})_{ff} \tag{50}$$

$$C_H = C_{H_r} + C_{H_c} \tag{51}$$

In equations (47) through (50), the shape factor has been used for consistency with equations (20b) and (22).

The detailed calculation procedure, including several simple auxiliary expressions that need no comment, is outlined in appendix D. The calculations were performed on an IBM 7094 electronic data processing machine.

RESULTS AND DISCUSSION

As outlined under "Construction of Data Curve," the initial meteor radius is that value of the assumed initial radius, r_b^*, which gives the most consistent results along with the best data fit. The data curves for various r_b^* are given in figure 1, and the resulting curves for variations of r_b with h for the various r_b^* (calculated as outlined above and in appendix D) are shown in figure 2. For r_b^* less than 20 cm, the radius appeared to increase

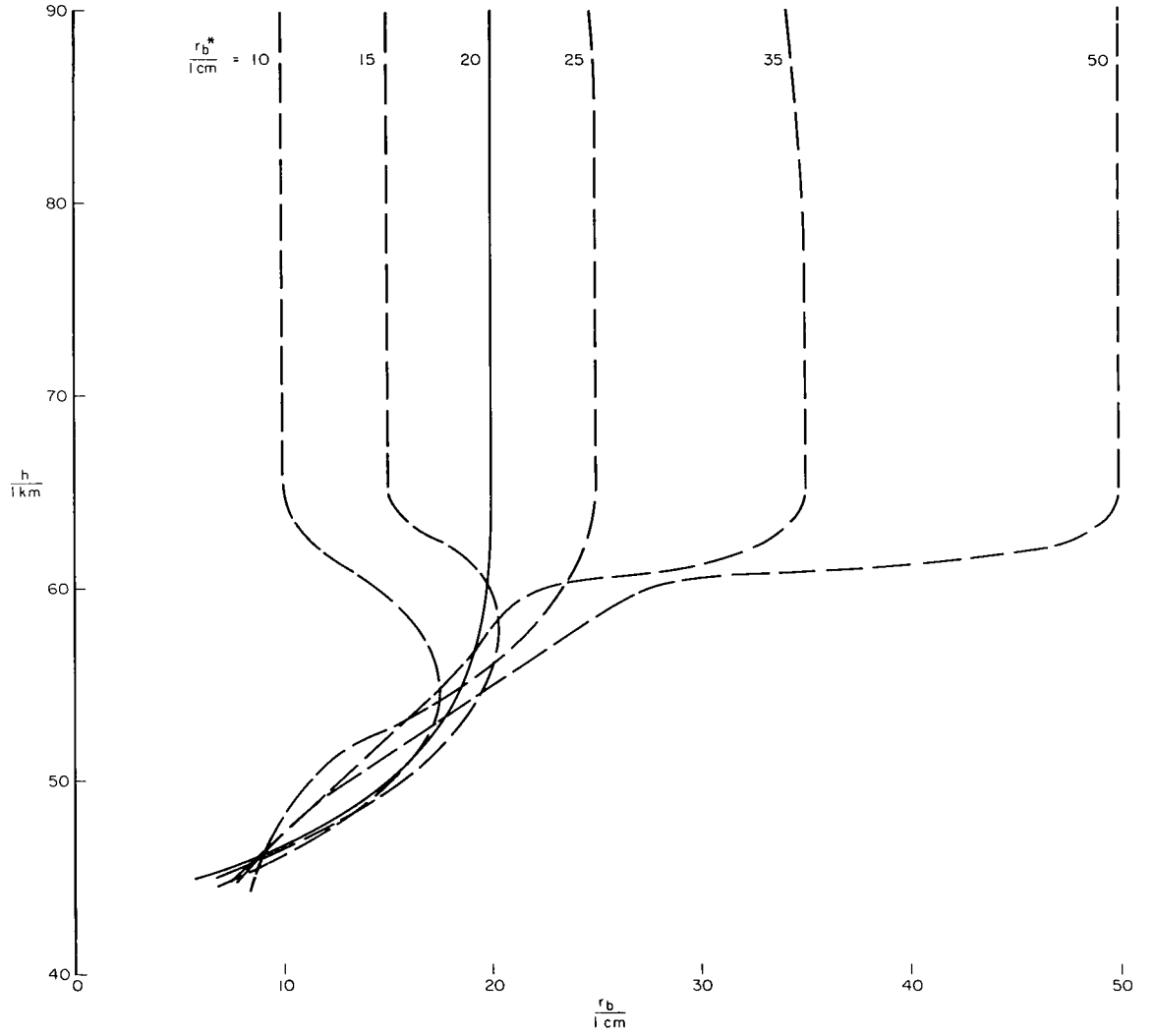

Figure 2.- Variation of meteor radius with altitude (s = 2).

before decreasing. For r_b^* greater than 25 cm, the data fit does not appear to be as good as for 20 cm. It appears that $r_b^* = 20$ cm gives the best results, so the remaining results given here correspond to $r_b^* = 20$ cm. (The data, listed in table V(c), are taken from figure 1(c).) Although the size of the main body of the meteor, before its fragmentation at lower altitudes, is very uncertain (see ref. 4), it is believed that the radius computed here is too low. This reflects, certainly, the approximate nature of these calculations and, probably, inaccuracy and uncertainties in the original meteor data. The results here would be improved if the shape factor, s, decreased from two toward unity with decreasing altitude, so that $C_{D_{eff}}$ would increase; r_b would then decrease more slowly and have a larger final value.

The results indicate that if the idealizations in this calculation are approximately valid, then the rapid variations of flow variables and high heat conduction characterizing a strong boundary shock wave were present in the ablating vapor flow of the Přibram meteor. This conclusion is indicated by: (1) the heat-conduction parameter, C_{h_c} (see fig. 3), is different from zero, (2) the ratios of conditions across the boundary shock wave (e.g., ρ_e/ρ_b; see fig. 4) are greater than unity, and (3) the vapor-flow Reynolds number, $\rho_b u_b d_i/\tilde{\mu}_b$ (where d_i and $\tilde{\mu}_b$ were estimated roughly; see appendix E), is much greater than unity. (For altitudes less than about 65 km, $\rho_b u_b d_i/\tilde{\mu}_b$ is of order 10^2 or greater; see appendix E.) The boundary shock wave is considered to be strong because of the large values of C_{h_c} and ρ_e/ρ_b. The calculated temperature change across the boundary shock wave on the Přibram meteor is small because the vapor ablates at low subsonic Mach number ($M_b = 1/3$) and because the density ratio across the boundary shock wave is high (see eq. (41)).

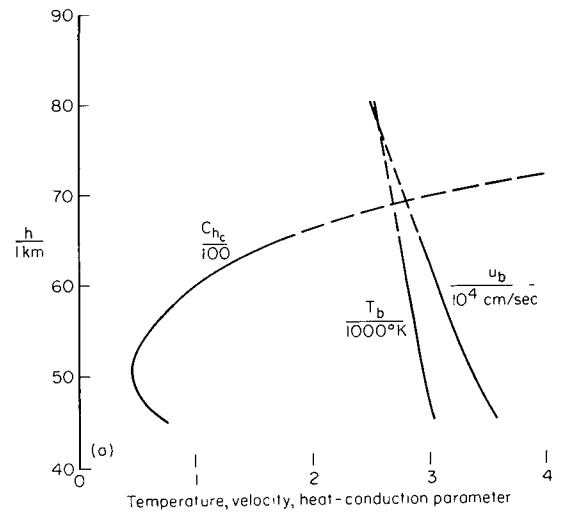

(a) Temperature, velocity, heat-conduction parameter.

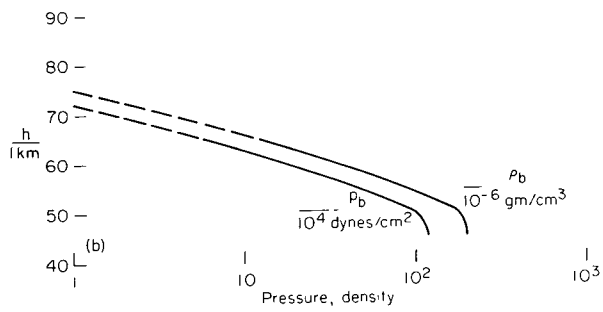

(b) Pressure, density.

Figure 3.- Vapor-flow variables at the meteor-vapor boundary ($r_b^* = 20$ cm, s = 2).

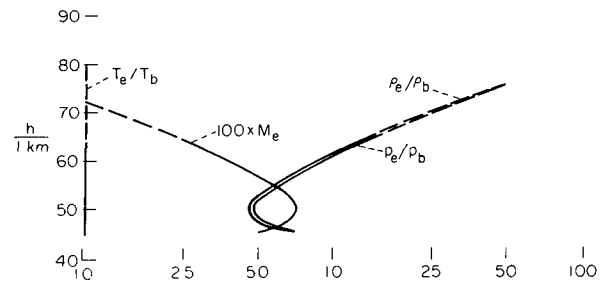

Figure 4.- Conditions across the boundary shock wave on the meteor ($r_b^* = 20$ cm, s = 2).

The validity of the equations used for the boundary shock wave depends on $Re_b \equiv \rho_b u_b d_i / \tilde{\mu}_b$ being large ($\gg 1$). The results that depend on the boundary-shock-wave theory are therefore not reliable much above 65 km altitude in these calculations for the Příbram meteor. In the calculations below 65 km altitude, for which Re_b is large, the vapor flow necessarily divides into thin viscous regions (the boundary shock wave and the interfacial layer) and an essentially inviscid region (see sketch (b)).[6] All viscous effects, including convective heat transfer, are absent from the inviscid region. Convective heat transfer from the hot compressed air is therefore confined to a thin layer at the interface; in the usual terminology of ablation theory, the convective heating is completely "blocked" from the body by the efflux of vapor. The only heat transfer from the outer layer of hot air behind the shock wave to reach the body is assumed to be that due to radiation. However, there is significant heat conduction in the vapor at the surface (within the thin boundary shock wave) that will be discussed below. Just as the boundary-shock-wave theory is not applicable at the beginning of the entry into the atmosphere, some point may be reached later where it is again not applicable. A point may be reached where the radius r_b has decreased to such an extent that (1) Re_b is decreased significantly because it contains a length proportional to r_b and (2) the radiation is much lower for smaller r_b so that the mass flux $\rho_b u_b$ contained in Re_b is also decreased significantly. Hence, when the radius becomes small, the vapor flow near the body may again approach a boundary-layer-type flow. This point in the trajectory of the Příbram meteor is below the lowest data point (see appendix E for values of Re_b), if it occurred at all. An additional effect of this phenomenon, when the radius becomes small enough and/or the velocity slow enough so that the ablation rate decreases considerably, is that the radius will decrease much slower; that is, the curve of radius versus altitude will at some point again become more nearly vertical in figure 2. This may be the effect beginning to show up in the curve for $r_b^* = 25$ cm in figure 2.

The primary meteor flight parameters of interest are the radius (fig. 2), the drag coefficients, and the heat-transfer coefficients (see figs. 5, 6, and 7). The first important result regarding drag to be noticed in figure 5 is that $C_{D_{eff}}$ remains, for all practical purposes, unity. (This depends, of course, on the shape factor being constant at 2.) Note, then, that one could ignore the boundary shock wave, assume $C_{D_{eff}} = 1.0$, and determine r_b from equation (13) (following the general procedure of Allen and James, ref. 3), using the most appropriate data curve for V and dV/dt versus altitude. The radius and $C_{D_{eff}}$ would then be known accurately, but not necessarily the heat transfer (see below) or the thermodynamic properties of the vapor. The second result regarding drag is that the viscous-compressive stress (at the vapor boundary) produces most of the effective drag, the thermodynamic

[6]Note that, even at 65 km altitude (taken to be the upper limit of validity of the theory), where the meteor radius was about 20 cm (fig. 2) and the thickness of the vapor layer was about 0.016 × 20 cm = 0.32 cm (see appendix E), the ratio of the boundary shock thickness to the entire vapor-layer thickness (ratio of order $1/Re_b$) was about 1/77, so the thickness of the boundary shock wave was about 0.32 cm × 1/77 = 0.00415 cm.

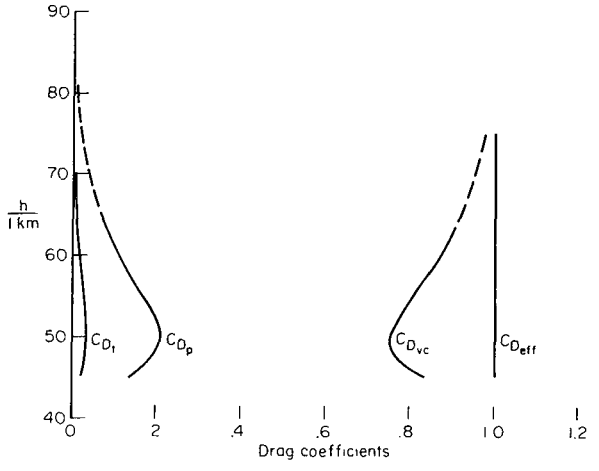

Figure 5.- Meteor drag coefficients (r_b* = 20 cm, s = 2).

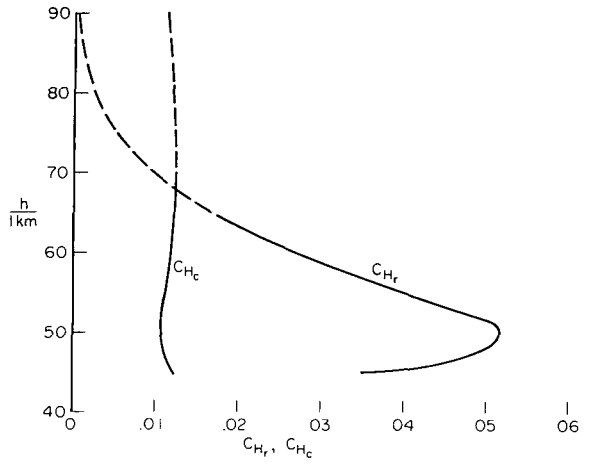

Figure 6.- Meteor heat-transfer coefficients (r_b* = 20 cm, s = 2).

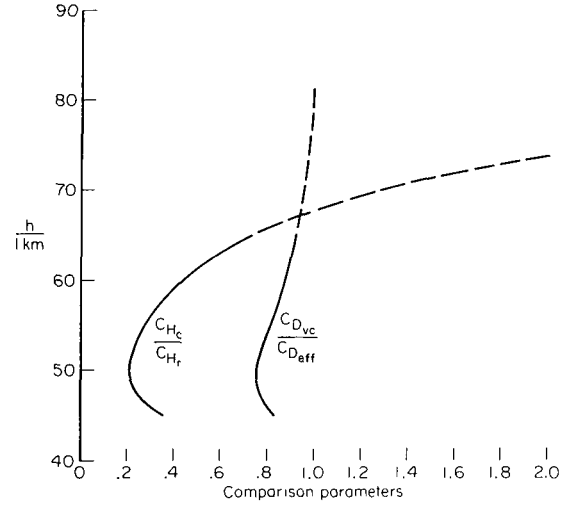

Figure 7.- Ratios showing boundary-shock effects (r_b* = 20 cm, s = 2).

pressure drag being generally much smaller and the retrothrust (represented by a "drag coefficient," C_{D_t}) practically negligible (see figs. 5 and 7). This result, that $C_{D_{vc}}$ is the most significant portion of $C_{D_{eff}}$ can be misleading, however. If the viscous-compressive stress were not included in the analysis, the pressure drag calculated would be much larger, since p_b would take the place of $p_b + (-\tau_b)$ in the momentum equation (eq. (23)).

The plot of the heat-transfer coefficients due to radiation and heat conduction in the vapor at the boundary (fig. 6) indicates that the heat conduction in the boundary shock wave plays a substantial role (see also fig. 7). To aid in understanding the roles of radiation and heat conduction at the surface, it is useful to consider equation (24). Assuming $\widetilde{Pr} = 1$, we have (see ref. 1):

$$q_{c_b} = \tau_b u_b \tag{52}$$

so that, from equation (24),

$$-q_r = \rho_b u_b \left(\zeta_{ab} + \frac{1}{2} u_b^2 \right) \tag{53}$$

From equations (53), (B15), and (B16) (or eqs. (74) in ref. 1), one sees that the radiative flux to the body, $-q_r$, contributes to: (1) heating the body material to vaporization temperature (by conduction within the body), (2) vaporizing the body material, and (3) increasing the kinetic energy of the vaporized material $[(1/2)u_b^2]$. Included in the energy of vaporization is the "flow energy," $p_b/\rho_b = RT_b$, added to the vaporized material. The latter term $[\rho_b u_b(p_b/\rho_b) = u_b p_b]$ is equivalent to the work required to blow off the vapor against the pressure p_b with velocity u_b. This energy, added by work, stays with the vapor as flow energy (giving the vapor an "enthalpy," $e + p/\rho$), since the force due to the thermodynamic pressure p is not dissipative. Now we see from equation (52), by analogy, that the contribution of the heat conduction back through the gas at the boundary, $-q_{c_b}$, is in the form of the work required to blow off the vapor against the viscous-compressive stress, $-\tau_b$, with velocity u_b. Since the force due to $-\tau_b$ is dissipative, however, no energy is added to the gas by this work, and it does not appear in equation (53).

For the heating, then, although the viscous effect (the heat conduction in the boundary shock wave) is large, one sees (as in the case of drag) that omitting the boundary shock wave from the analysis would not influence the overall results as much as might at first be supposed. The heat conduction simply balances the work of blowing off the vapor against the viscous-compressive stress (assuming $\widetilde{Pr} = 1$).

Although detailed flow calculations would be affected significantly by the boundary shock wave, an important result here is that, for overall gross effects, ignoring the boundary shock wave and assuming $C_{D_{eff}}$ to be unity and the heat load producing the vaporization to be just the radiation from the hot gas, one should obtain good approximate results. The only difficulty remaining in ignoring the boundary shock wave is in determining the ablation temperature, which also determines ζ_{ab}. However, since the largest part of ζ_{ab} is comprised of the heat of vaporization, ζ_{ab} is not too strongly dependent on the vaporization temperature. The approximate equations used by Allen and James (ref. 3) therefore give good approximate results for the overall motion and heating of a meteor (especially since their assumed values of ζ_{ab} and T_b are approximately correct for the most critical part of the trajectory), even though the boundary shock wave has not previously been considered. The most important conclusion here is that detailed flow calculations, both for determining the flow characteristics and for computing more precise results on the motion and heating of the meteoric body, should consider the possible effects of the boundary shock wave. In the case of the Příbram meteor, the boundary shock effects on the flow are indicated by the idealized theory to be substantial.

CONCLUDING REMARKS

The results of including a boundary shock wave in a simplified calculation of the flight parameters of a stone-meteoric fireball have been

studied using meteor-tracking data for the analysis. The results found or deduced are enumerated explicitly, and then elaborated upon, in summary of the above discussion. They include:

(a) the calculated values of ratios (which represent the "jumps" or rapid variations) of vapor-flow parameters across the boundary shock wave, and values of other parameters in the vapor that relate to the boundary shock wave;

(b) qualitative differences in values of the vapor-flow parameters from values that would be obtained by ignoring the possible presence of the boundary shock wave (these differences can be inferred from the results (a), but were also checked in a simple calculation, not shown);

(c) the significance of (a) and (b) to the vapor flow field;

(d) the calculated values of the flight parameters, including the meteor radius and the various heat-transfer coefficients and drag coefficients;

(e) qualitative differences in the calculated values of the overall flight parameters from values that would be obtained by ignoring the possible presence of the boundary shock wave; and

(f) significance of the above results (of including the boundary shock wave in the present calculation of meteor flight parameters) to more detailed analyses of the flight parameters.

The calculations indicate that, if the idealizations made are valid, conditions were present in the ablating-vapor flow of the Ondřejov meteor Příbram for a strong boundary shock to occur according to the boundary-shock-wave theory presented previously.

During the portion of the Příbram meteor trajectory for which tracking data were obtained and for which the boundary-shock-wave theory is presumed to apply (between about 65 and 45 km altitude) the results are: (1) neither the pressure ratio nor the density ratio across the boundary shock wave was ever less than about 4.5, (2) the temperature change was about 2 percent across the boundary shock, (3) the viscous-compressive drag was always at least 75 percent of the total effective drag, (4) the total effective drag coefficient remained nearly constant at the value unity, and (5) heat transfer by conduction at the surface in the vapor was always at least 20 percent as large as the radiative heat transfer.

Since the density a short distance from the molten surface, ρ_e, is significantly different from ρ_b, which in turn is fairly close to the density that would be calculated by ignoring the possible presence of a boundary shock (or equivalently by omitting the translational-nonequilibrium condition on the vaporization rate), the calculated effects on the vapor flow are substantial. Therefore a more detailed analysis of the flight parameters that would use a detailed flow field analysis (for more precise calculation or for other

reasons) should include consideration of a boundary shock wave, under the conditions where its presence in significant strength is expected.

The results of the analysis including the boundary shock wave indicate an initial radius between 20 and 25 cm, probably closer to 20 cm, for the meteor. The actual initial radius is believed to have been somewhat larger than this. The difference is probably due to the approximations made in the analysis and to uncertainties in the original meteor data.

If the boundary shock wave were not considered in calculating the overall gross flight parameters (so that virtually all of the heating would be assumed to be by radiation and most of the drag due to pressure), it is still possible to obtain realistic approximate results for the overall motion and heating of the meteoric body by judicious choice of: (1) assumed values of the effective drag coefficient ($C_{D_{eff}}$), the temperature of vaporization (T_b), and the total energy required to heat and vaporize a unit mass of the meteoric material (ζ_{ab}) (as used effectively by Allen and James) and (2) a suitable curve representing the meteor-tracking data. Thus, although the occurrence of a boundary shock wave may be important to the flow details, the overall flight characteristics of the meteor (in the class expected to have a boundary shock) are not too significantly affected by the presence of a boundary shock wave if proper estimates are made, as done by Allen and James.

Ames Research Center
National Aeronautics and Space Administration
Moffett Field, Calif., 94035, Jan. 31, 1967
124-07-02-23-00-21

APPENDIX A

PRINCIPAL NOTATION

A	cross-sectional area of the body
$C_{D_{eff}}$	effective drag coefficient; equations (11), (22), and (26)
C_{D_p}	coefficient of drag due to pressure, equation (47)
C_{D_t}	contribution to total $C_{D_{eff}}$ due to retrothrust of vapor, equation (49)
$C_{D_{vc}}$	coefficient of drag due to viscous compressive stress, equation (48)
C_{H_c}	coefficient of heat transfer by conduction, equations (32) and (50)
C_{h_c}	conduction coefficient defined by equation (31)
C_{H_r}	coefficient of heat transfer by radiation; equations (9), (20b), and (26)
c	specific heat
c_p, c_v	specific heats in gas (vapor) at constant pressure and constant volume
$\overline{D}$	shock standoff function defined by equation (4)
d_i	distance from body to interface between vapor and air
d_o	distance from interface to shock wave, that is, thickness of outer shock layer
dE, dH, dW	differential quantities first used in equation (B10)
$d\eta, d\xi$	differential quantities defined prior to equation (B1)
e	specific internal energy
f	total force per unit area acting on an elemental surface
$\tilde{f}$	body force per unit mass acting in the direction of motion; $\tilde{f} = g \sin \theta$ when $\varphi = gh$
g	acceleration of gravity

h	altitude above the earth's surface
I	rate of energy radiation per unit volume in the outer shock layer
K_1, K_2	constants defined by equations (C5) or (C6)
K_1', K_2'	constants of integration first used in equations (C9) and evaluated in (C11) or (C12)
k	thermal conductivity
$\tilde{k}$	shock density ratio, ρ_∞/ρ_2
L_f	latent heat of fusion
L_v	latent heat for vaporization at low rate
M	Mach number
m	mass of meteor
$\tilde{m}$	portion of body mass between x_a and $x = 0$ at a given time
$\mathcal{m}$	molecular weight of vapor
p	pressure
Pr	Prandtl number, $\mu c_p/k$
$\widetilde{Pr}$	Prandtl number based on $\tilde{\mu}$, $\tilde{\mu}c_p/k$
Q_r	total radiative heating rate to a flat-face body
q	heat flux (positive to the left in sketches (a) and (b), positive to the right in sketches (d) and (e))
q_c	conduction heat flux
q_r	radiative heat flux
R	gas constant (universal gas constant divided by molecular weight)
Re_b	vapor-ablation Reynolds number, $\rho_b u_b d_i/\tilde{\mu}_b$
r_b	body radius, sketch (a)
r_b^*	assumed initial radius of meteor
r_i	distance from center of nearly spherical body to vapor-air interface, sketch (a)
s	shape factor, equations (21)

T	temperature
t	time
u	velocity of vapor relative to molten meteor surface (to the right in sketch (d))
V	magnitude of meteor velocity relative to the earth
V^*	approximate value of meteor velocity at atmosphere entry
v_b	velocity of vapor at the molten surface relative to the body mass whose velocity is V; $u_b - u_s$
x	coordinate in the direction of the body motion whose origin is fixed at the receding molten surface, sketch (d)
x'	coordinate in the direction of the body motion whose origin is fixed in space
Z,Z'	$\frac{VC_{H_r}}{C_{D_{eff}}}$, equations (14) and (35)
α	$\frac{\rho_b}{\rho_e}$, equation (39)
β_1,β_2	constants defined by equations (C4)
γ	ratio of specific heats, $\frac{c_p}{c_v}$
ζ_{ab}	$e_b - e_a + RT_b$, equations (B15) and (B16)
θ	angle between velocity vector and equipotential surface (e.g., earth's surface when $\varphi = gh$)
λ	function of $\tilde{k}$ and $\bar{D}$, equation (6)
μ	shear-viscosity coefficient
$\tilde{\mu}$	defined in equation (28)
ρ	mass density per unit volume
ρ_m	mass density of meteor
ρ_{SL}	atmospheric density at sea level, equation (2)
$\bar{\rho}$	altitude-density function, equation (1)

σ	$Z - Z'$
τ	viscous compressive stress
φ	body-force potential; for gravitational force $\varphi = gh$, equation (B4b)
ψ	variable quantity on meteor surface, equation (17)
ψ_o	constant value of ψ on a flat-face body

Subscripts

a	in general, an arbitrary point in $x < 0$; in particular, value where $k \frac{dT}{dx} \approx 0$, that is, where T_a is the cold interior temperature
b	value at the boundary in the vapor ($x = 0^+$)
e	value outside the boundary shock wave in the vapor
f	value at fusion, that is, where $T = T_f$, the fusion temperature
ff	value on flat-face body
liq	value in the liquid (molten meteoric material)
o	value at the stagnation point, on the air-vapor interface
ref	arbitrary reference value
s	value at the molten surface, inside the surface ($x = 0^-$)
sol	value in the solid meteoric material
2	value behind the shock wave, sketch (b)
∞	condition in the ambient atmosphere at altitude h

APPENDIX B

DERIVATION OF THE ONE-DIMENSIONAL CONSERVATION EQUATIONS

A derivation of the equations of conservation of mass, momentum, and energy is presented for an accelerating body with the following conditions: A rapid efflux of vapor from the forward face of the body is produced by vaporization of the body material due to absorption at the body surface of intense radiation. All motion, including that of the body and the vapor, is assumed to be one-dimensional. The body has a cross-sectional area A and an instantaneous mass m. The gas in front of the body is the outflowing vapor. The effects of any gas to the rear are neglected. The body is moving in a force field of potential φ. (In the case of gravitational force, $\varphi = gh$.)

For the following development, refer to sketch (d), where all motion is to the right. Let

$V = V(t)$ be the instantaneous velocity of the body;

x be a coordinate in the direction of the body motion whose origin is always fixed at the receding surface;

x' be a coordinate in the direction of the body motion whose origin is fixed in space (e.g., with respect to the earth's surface);

$u_s = u_s(t)$ be the rate at which the surface is receding into the body mass, that is, the velocity in the $-x$ direction of the surface relative to the internal mass of the body. (Thus, the absolute velocity of the surface is $V - u_s$.);

$u_b = u_b(t)$ be the velocity of the gas (vapor) at the surface relative to the surface. (The absolute instantaneous velocity of the gas at the surface is $u_b - u_s + V$.); and

$u = u(x,t)$ be the instantaneous velocity of the gas to the right relative to the surface at a distance x from the surface. (The absolute velocity of the gas at x,t is $u - u_s + V$.).

Note that, relative to the x coordinate, the surface is stationary, the mass inside the body is moving with velocity u_s, the gas is moving with velocity u, and the surface value is u_b. (Relative to the x' coordinate, the body has velocity $V = dx'/dt$.) (Subscript b refers to values in the gas at the boundary of the gas flow ($x = 0^+$); subscript s refers to values inside the unvaporized material at the surface ($x = 0^-$); subscript a refers to an arbitrary point a inside the surface ($x < 0$).)

Consider the motion of the system of constant mass $\tilde{m}$ during the infinitesimal time interval dt between t_o and $t_o + dt$, where $\tilde{m}$ is the portion of the body mass m between x_a and $x = 0$ at time t_o. The mass

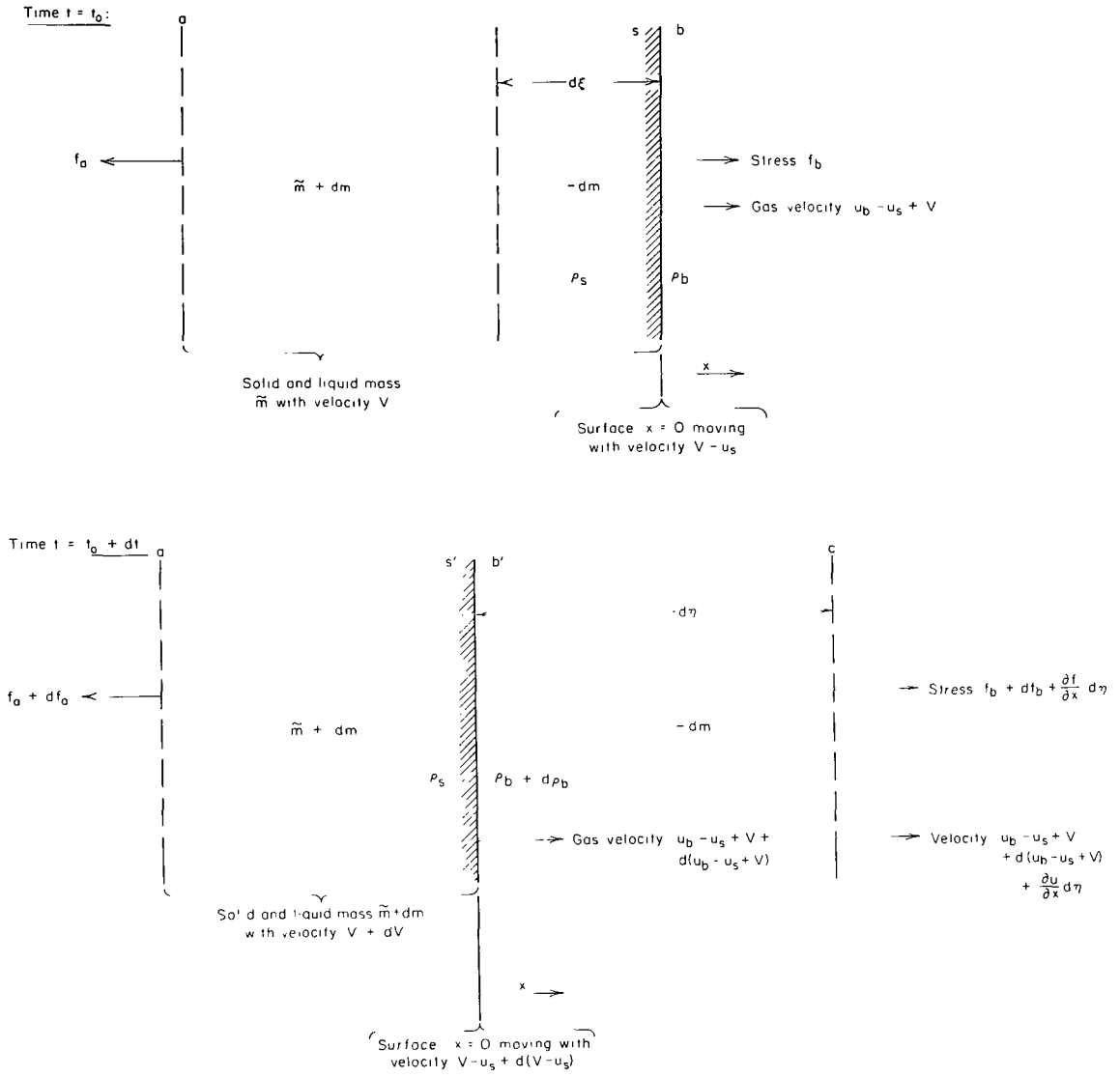

Sketch (d).- Ablation of surface during time interval dt.

vaporized during dt is -dm. (Although -dm is lost from the "body" during dt, it remains part of our "closed," or constant mass, system.) Let $d\xi$ be the dimension of the mass -dm before it is vaporized and $d\eta$ its dimension after it is vaporized; thus,

$$-dm = \rho_s A \, d\xi = \rho_b A \, d\eta \tag{B1}$$

where, by definition,

$$u_s = \frac{d\xi}{dt} , \qquad u_b = \frac{d\eta}{dt} \tag{B2}$$

From equations (B1) and (B2) we have a convenient statement of conservation of mass:

$$-\frac{dm}{dt} = A\rho_s u_s = A\rho_b u_b \tag{B3}$$

In the following an appropriate "momentum equation" is derived from the principle of conservation of momentum. First, define f to be the sum of "surface forces" per unit area (such as pressure and viscous stress in the gas or liquid, and tensile or compressive stress in the solid). Positive values of f indicate tension, so that, in the gas or liquid,

$$f = -p + \tau \tag{B4a}$$

where p is the thermodynamic pressure and τ the viscous-compressive stress ($\tau = \tilde{\mu}(du/dx)$; see, e.g., ref. 16, p. 331, or ref. 1). Also, define $\tilde{f}$ to be the body force per unit mass acting on the mass $\tilde{m}$ in the direction of the body motion, that is,

$$\tilde{f} = -\frac{d\varphi}{dx'} \tag{B4b}$$

(In the case where the potential is $\varphi = gh$,

$$\tilde{f} = g \sin\theta$$

where

$$\sin\theta = -\frac{dh}{dx'} = -\frac{dh}{V\,dt}$$

i.e., where θ is the angle between the trajectory of the body motion and an equipotential surface, such as the earth's surface.) The average external force to the right (sketch (d)) acting on the mass $\tilde{m}$ during dt is then

$$\tilde{m}\tilde{f} + \frac{1}{2}A\left[(f_b - f_a) + \left(f_b + df_b + \frac{\partial f}{\partial x}\,d\eta\right) - (f_a + df_a)\right]$$

$$= \tilde{m}\tilde{f} + A(f_b - f_a) + \text{higher order terms}$$

so that the impulse during dt is

$$\tilde{m}\tilde{f}\,dt + A(f_b - f_a)dt \tag{B5}$$

The momentum change (to the right) of the mass $\tilde{m}$ during dt is

$$(\tilde{m} + dm)(V + dV) + (-dm)\left[u_b - u_s + V + d(u_b - u_s + V) + \frac{1}{2}\frac{\partial u}{\partial x}\,d\eta\right] - \tilde{m}V$$

$$= \tilde{m}\,dV - (u_b - u_s)dm + \text{higher order terms} \tag{B6}$$

Neglecting the higher order differentials, we may then write, from the principle of conservation of momentum,

$$A(f_b - f_a)dt + \tilde{m}\tilde{f}\,dt = \tilde{m}\,dV - (u_b - u_s)dm \tag{B7a}$$

Convenient forms for this equation are

$$-\frac{\tilde{m}}{A}\left(\frac{dV}{dt} - \tilde{f}\right) = f_a - f_b + (u_b - u_s)\left(-\frac{1}{A}\frac{dm}{dt}\right) \tag{B7b}$$

and, with use of equation (B3),

$$\rho_s u_s^2 - \left(f_a + \frac{\tilde{m}}{A}\frac{dV}{dt} - \frac{\tilde{m}}{A}\tilde{f}\right) = \rho_b u_b^2 - f_b \tag{B7c}$$

If we take point a as the back surface of the body, where $f_a = 0$ and $\tilde{m} = m$, we have, using equations (B3) and (B4) in (B7b),

$$-\frac{m}{A}\left(\frac{dV}{dt} - \tilde{f}\right) = \rho_b u_b^2\left(1 - \frac{\rho_b}{\rho_s}\right) + p_b - \tau_b \tag{B8a}$$

in which, of course, $\rho_b/\rho_s \ll 1$ and may be neglected. Another convenient form for equation (B8a) is

$$-m\left(\frac{dV}{dt} - \tilde{f}\right) = D_p + D_{vc} + F_T \tag{B8b}$$

where the pressure drag, the viscous-compressive drag, and the retrothrust due to ejected vapor are, respectively,

$$\left.\begin{aligned} D_p &= p_b A \\ D_{vc} &= -\tau_b A \\ F_T &= -\frac{dm}{dt}(u_b - u_s) = -\frac{dm}{dt}v_b \\ &= \rho_b u_b^2 A\left(1 - \frac{\rho_b}{\rho_s}\right) \approx \rho_b u_b^2 A \end{aligned}\right\} \tag{B9}$$

where $v_b = u_b - u_s$ is the gas velocity relative to the body mass whose velocity is V.

To derive an equation representing conservation of energy, we begin with the first law of thermodynamics applied to the closed system of mass $\tilde{m}$ during dt (see above definitions and sketch (d)):

$$dE = dH + dW \tag{B10}$$

where

dE = the change in energy of the system of mass $\tilde{m}$ during dt

dH = the net heat added to the system of mass $\tilde{m}$ during dt

dW = the work done on the system of mass $\tilde{m}$ by external forces during dt

The energy E possessed by the mass $\tilde{m}$ is composed of internal energy, kinetic energy, and potential energy. Let e denote internal energy per unit mass at a certain point in the mass $\tilde{m}$ at time $t = t_o$ and $e + de$ be the corresponding value at time $t_o + dt$. Also, denote the latent heat of fusion and latent heat of vaporization at low rates (see appendix B of ref. 1) by L_f and L_v, respectively. Refer to sketch (e). During dt the surface, $x = 0$,

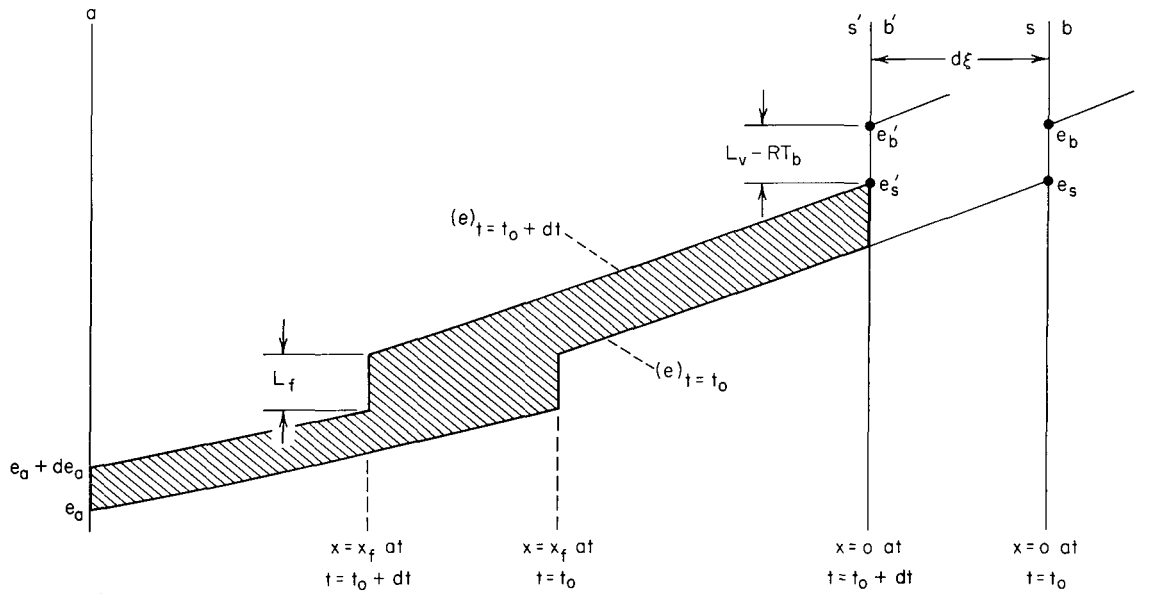

Sketch (e).- Change of specific-internal-energy distribution in body during time interval dt.

where the vaporization is taking place, recedes from s to s', a distance $d\xi$ relative to the internal body mass. For simplicity, changes in e_s and e_b with time are neglected, that is, $e_{s'} \approx e_s$ and $e_{b'} \approx e_b$. Then, during dt, the internal energy curve is simply shifted a distance $d\xi$ to the left in sketch (e). Neglecting higher order differentials, one finds the shaded area to be

$$(e_s - e_a)d\xi$$

Since the mass included between point a and point s' is $\tilde{m} + dm$, the change in internal energy of the mass $\tilde{m} + dm$ during dt is

$$\rho_s A(e_s - e_a)d\xi \equiv -dm(e_s - e_a) \tag{B11}$$

Note that this takes into account a phase change (fusion) at $x = x_f$ where the fusion temperature is T_f; thus, if the specific heats in the solid and liquid are constants c_{sol} and c_{liq}, one may write

$$e_s - e_a = c_{sol}(T_f - T_a) + L_f + c_{liq}(T_s - T_f) \tag{B12}$$

At $t = t_o$, the mass $(-dm)$ has an internal energy of

$$-dm\left(e_s - \frac{1}{2}\frac{de}{dx}\,d\xi\right) + \text{higher order terms}$$

and at $t = t_o + dt$ the mass $(-dm)$ has an internal energy of

$$-dm\left(e_b + \frac{1}{2}\frac{de}{dx}\,d\eta\right) + \text{higher order terms}$$

so that, with neglect of higher order differentials, the change in internal energy of the mass $(-dm)$ is

$$-dm(e_b - e_s) \tag{B13}$$

Thus, from equations (B11) and (B13), the total change in internal energy of the mass $\tilde{m}$ during dt is

$$-dm(\zeta_{ab} - RT_b) \tag{B14}$$

where

$$\zeta_{ab} - RT_b \approx e_b - e_a \tag{B15}$$

(see appendix B of ref. 1). For constant specific heat in the solid, liquid, and constant-temperature phase changes (e.g., see ref. 19), if point a is to the left of the fusion point, then

$$\zeta_{ab} = c_{sol}(T_f - T_a) + L_f + c_{liq}(T_b - T_f) + L_v\,, \qquad (x_a < x_f) \tag{B16}$$

In sketch (d), the kinetic energy of $\tilde{m}$ at t_o is $(1/2)\tilde{m}V^2$. At time $t_o + dt$ the kinetic energy of the mass $\tilde{m} = (\tilde{m} + dm) + (-dm)$ is

$$\frac{1}{2}(\tilde{m} + dm)(V + dV)^2 + \frac{1}{2}(-dm)\left[(u_b - u_s + V) + d(u_b - u_s + V) + \frac{1}{2}\frac{\partial u}{\partial x}\,d\eta\right]^2$$

Therefore, the total change in kinetic energy of the mass $\tilde{m}$ during dt (omitting higher order differentials) is

$$\tilde{m}V\,dV + (-dm)\left[V(u_b - u_s) + \frac{1}{2}(u_b - u_s)^2\right] \tag{B17}$$

From expressions (B14), (B17), and the expression for the potential-energy change:

$$\tilde{m}\, d\varphi = -\tilde{m}\tilde{f}\, dx' = -\tilde{m}\tilde{f}V\, dt$$

we then have

$$dE = \tilde{m}V\, dV + (-dm)\left[\zeta_{ab} - RT_b + \frac{1}{2}(u_b - u_s)^2 + V(u_b - u_s)\right] - \tilde{m}V\tilde{f}\, dt \qquad (B18)$$

The net heat added to the system of mass $\tilde{m}$ during dt is

$$dH = (q_a - q_b)A\, dt \qquad (B19)$$

where q denotes heat flux to the right in sketch (d) and where

$$\left.\begin{aligned} q_a &= -(k\, dT/dx)_a \\ q_b &= q_r + q_{c_b} = q_r - (k\, dT/dx)_b \end{aligned}\right\} \qquad (B20)$$

and $-q_r$ is the radiative heat from the right that is absorbed at $x = 0$ and q_{c_b} the heat flux by conduction in the vapor at the boundary ($x = 0^+$).

The work done on the system of mass $\tilde{m}$ during dt by the gas in front of it is the product of the average force during dt on the forward bounding surface times the distance through which that surface is moved. From sketch (d) one finds that the forward bounding surface of the mass $\tilde{m}$ moves, during dt, from b to c, an actual distance of

$$(u_b - u_s + V)dt + \text{higher order terms}$$

Thus, the work done on $\tilde{m}$ during dt by the gas in front is

$$f_b A(u_b - u_s + V)dt + \text{higher order terms} \qquad (B21)$$

Similarly, the work done on $\tilde{m}$ during dt by the mass behind $\tilde{m}$ is

$$-f_a AV\, dt + \text{higher order terms} \qquad (B22)$$

and the total work done on mass $\tilde{m}$ during dt, with neglect of the higher order terms, is then

$$dW = (f_b - f_a)AV\, dt + f_b(u_b - u_s)A\, dt \qquad (B23)$$

The first law of thermodynamics, equation (B10), written in the form

$$\frac{dH}{dt} = \frac{dE}{dt} - \frac{dW}{dt} \qquad (B24)$$

and with use of the expressions (B18), (B19), and (B23), gives an equation expressing conservation of energy:

$$q_a - q_b = \frac{\tilde{m}}{A} V \left(\frac{dV}{dt} - \tilde{f} \right) - \frac{1}{A} \frac{dm}{dt} \left[\zeta_{ab} - RT_b + \frac{1}{2} (u_b - u_s)^2 + V(u_b - u_s) \right]$$

$$+ (f_a - f_b)V - f_b(u_b - u_s) \tag{B25}$$

Substitution of the momentum equation (B7b) into (B25) yields

$$q_a - q_b = - \frac{1}{A} \frac{dm}{dt} \left[\zeta_{ab} - RT_b + \frac{1}{2} (u_b - u_s)^2 \right] - f_b(u_b - u_s) \tag{B26}$$

Another useful form obtainable from equation (B25) with substitution of (B3), (B7c), and (B15) is

$$\rho_b u_b e_b + \frac{1}{2} \rho_b u_b^3 + q_b - u_b f_b = \rho_s u_s e_a + \frac{1}{2} \rho_s u_s^3 + q_a - u_s \left(f_a + \frac{\tilde{m}}{A} \frac{dV}{dt} - \frac{\tilde{m}}{A} \tilde{f} \right) \tag{B27}$$

If we now take point a far enough back from the body surface that q_a is negligible and T_a is the cold interior temperature, using equations (B3) and (B4), we may write (B26) in the following two convenient forms:

$$-(q_r + q_{c_b}) = \rho_b u_b \left[\zeta_{ab} - RT_b + \frac{1}{2} u_b^2 \left(1 - \frac{\rho_b}{\rho_s} \right)^2 \right] + (p_b - \tau_b) u_b \left(1 - \frac{\rho_b}{\rho_s} \right) \tag{B28}$$

where, as in equation (B8a), $\rho_b/\rho_s \ll 1$ and may be neglected; or

$$\frac{dH}{dt} = - \frac{dm}{dt} \left(\zeta_{ab} - RT_b + \frac{1}{2} v_b^2 \right) + (D_p + D_{vc}) v_b \tag{B29}$$

where $dH/dt = -q_b A = -(q_r + q_{c_b})A$; $v_b = u_b - u_s$, the gas velocity relative to the body mass whose velocity is V; D_p and D_{vc} are given by equation (B9), dm/dt is given by equation (B3); and ζ_{ab} is given by equation (B16), with T_a as the cold interior temperature.

Following is an interpretation of equation (B29): The effects of the heat transfer dH during the time interval dt are: (a) to add internal energy to vaporize the mass $(-dm)$ and raise the temperature of an equivalent mass to the level that $(-dm)$ had before being vaporized (this accounts for the term $-dm(\zeta_{ab} - RT_b)$; (b) to add kinetic energy to $(-dm)$ relative to its original motion $[(1/2)(-dm)v_b^2]$; and (c) to blow off vapor with force $(D_p + D_{vc})$ acting through distance $v_b dt$ relative to the body motion $[(D_p + D_{vc})v_b\, dt]$.

In this derivation of the equations of motion and heating, note specifically that the following are accounted for:

(1) heat transfer into the body, as well as heat transfer used to vaporize the surface material;

(2) work done to blow off vapor, as well as the kinetic, potential, and internal energy possessed by the outflowing vapor;

(3) recession of the ablating surface;

(4) drag due to the viscous compressive stress, as well as pressure drag, retrothrust of ejected vapor, and the gravitational force;

(5) heat conduction associated with the viscous stress, as well as radiative heating.

APPENDIX C

ADDITIONAL RESULTS FROM CONSERVATION EQUATIONS

In addition to the conservation equations themselves, some interesting and useful side results can be obtained from the above derivation of the conservation equations. The energy equation presented above, in its complete form, can be used to calculate the heat transfer and the temperature distribution in the body, including the depth of the layer of molten stone and the depth at which the solid stone receives significant heating.

For this purpose, equation (B26) may be written (neglecting ρ_b/ρ_s in comparison to unity) as

$$-\left(\frac{k\,dT}{dx}\right)_a = q_{c_b} + q_r + \rho_b u_b \left(\zeta_{ab} - RT_b + \frac{1}{2} u_b^2\right) + (p_b - \tau_b)u_b \qquad (C1)$$

in which point a is arbitrary, so that

$$\left.\begin{aligned} \zeta_{ab} &= c_{sol}(T_f - T_a) + L_f + c_{liq}(T_b - T_f) + L_v\,, \qquad (x_a \le x_f) \\ \zeta_{ab} &= c_{liq}(T_b - T_a) + L_v\,, \qquad (x_f \le x_a \le 0) \end{aligned}\right\} \qquad (C2)$$

Then equation (C1) becomes

$$(dT/dx) - \beta_1(T - K_1) = 0\,, \qquad (x \le x_f) \qquad (C3a)$$

$$(dT/dx) - \beta_2(T - K_2) = 0\,, \qquad (x_f \le x \le 0) \qquad (C3b)$$

where

$$\beta_1 \equiv \frac{\rho_b u_b c_{sol}}{k_{sol}}\,, \qquad \beta_2 \equiv \frac{\rho_b u_b c_{liq}}{k_{liq}} \qquad (C4)$$

$$\beta_1 K_1 = \frac{1}{k_{sol}}\left\{q_{c_b} + q_r + \rho_b u_b \left[c_{sol}T_f + L_f + c_{liq}(T_b - T_f) + L_v - RT_b + \frac{1}{2} u_b^2\right] + (p_b - \tau_b)u_b\right\} \qquad (C5a)$$

$$\beta_2 K_2 = \frac{1}{k_{liq}}\left\{q_{c_b} + q_r + \rho_b u_b \left[c_{liq}T_b + L_v - RT_b + \frac{1}{2} u_b^2\right] + (p_b - \tau_b)u_b\right\} \qquad (C5b)$$

Much simpler expressions for K_1 and K_2 than equations (C5) can be obtained as follows: Take point a far enough back from the surface so that q_a is small and T_a is the cold interior temperature. Then, as $x \to -\infty$, $T \sim T_a$ and $dT/dx \to 0$; K_1 is found (from eq. (C3a)) to be

$$K_1 = T_a \tag{C6a}$$

Further, equations (C4) through (C6a) can be combined to give

$$K_2 = \frac{k_{sol}}{k_{liq}} \frac{\beta_1}{\beta_2} K_1 - \frac{\rho_b u_b}{\beta_2 k_{liq}} [(c_{sol} - c_{liq})T_f + L_f]$$

$$= T_f - \frac{c_{sol}}{c_{liq}} (T_f - T_a) - \frac{L_f}{c_{liq}} \tag{C6b}$$

The boundary condition for equation (C3b) is

$$x = 0 , \quad T = T_b \tag{C7}$$

Since T_f is known, the location x_f will be determined by solving equation (C3b) for the condition

$$x = x_f , \quad T = T_f \tag{C8a}$$

The boundary condition for equation (C3a) is then

$$x = x_f , \quad T = T_f \tag{C8b}$$

The solutions to equations (C3a) and (C3b) are

$$T = K_1 + K_1' e^{\beta_1 x} , \quad (x \leq x_f) \tag{C9a}$$

$$T = K_2 + K_2' e^{\beta_2 x} , \quad (x_f \leq x \leq 0) \tag{C9b}$$

Substitution of the boundary conditions gives

$$\left.\begin{aligned} T_b &= K_2 + K_2' \\ T_f &= K_2 + K_2' e^{\beta_2 x_f} \\ T_f &= K_1 + K_1' e^{\beta_1 x_f} \end{aligned}\right\} \tag{C10}$$

from which the expressions for K_2', K_1', and x_f are obtained:

$$\left.\begin{aligned} K_2' &= T_b - K_2 \\ x_f &= \frac{1}{\beta_2} \log\left(\frac{T_f - K_2}{T_b - K_2}\right) \\ K_1' &= (T_f - K_1)\left(\frac{T_f - K_2}{T_b - K_2}\right)^{-\beta_1/\beta_2} \end{aligned}\right\} \qquad (C11)$$

Note also that

$$\left.\begin{aligned} K_1' &= (T_f - K_1)e^{-\beta_1 x_f} \\ K_2' &= (T_f - K_2)e^{-\beta_2 x_f} \end{aligned}\right\} \qquad (C12)$$

and that the distribution (C9) can be written conveniently as:

$$\left.\begin{aligned} \frac{T - K_1}{T_f - K_1} &= e^{\beta_1(x-x_f)}, \quad (x \le x_f) \\ \frac{T - K_2}{T_f - K_2} &= e^{\beta_2(x-x_f)}, \quad (x_f \le x \le 0) \end{aligned}\right\} \qquad (C13)$$

where

$$\left.\begin{aligned} K_1 &= T_a \\ K_2 &= T_f - \frac{c_{sol}}{c_{liq}}(T_f - T_a) - \frac{L_f}{c_{liq}} \\ x_f &= \frac{1}{\beta_2} \log\left(\frac{T_f - K_2}{T_b - K_2}\right) \end{aligned}\right\} \qquad (C14)$$

and where β_1 and β_2 are given by equations (C4). Thus, the temperature distribution in the body is determined (eqs. (C13)), as well as the depth of the molten layer, $-x_f$ (eqs. (C14)). The depth of the solid stone material receiving significant heating can be observed from the temperature distribution, or one can calculate the depth at which the temperature is, say, 1 percent higher than the cold interior temperature. If one calls this depth $-x_c$ and the temperature T_c, the first of equations (C13) gives

$$\frac{T_c - K_1}{T_f - K_1} = e^{\beta_1(x_c - x_f)}$$

from which

$$x_c = x_f + \frac{1}{\beta_1} \log\left(\frac{T_c - K_1}{T_f - K_1}\right) \qquad (C15)$$

where, for example, $T_c = 1.01\ T_a$.

To compute the temperature distributions, one needs to know values for k_{sol} and k_{liq}, in addition to the constants listed in table II. Öpik gives a value for thermal conductivity of meteoric stone as 2×10^5 erg/cm sec °K (ref. 12, p. 162). We take this to be

$$k_{sol} = 2 \times 10^5 \text{ erg/cm sec } ^\circ\text{K}$$

In general, the ratio k_{liq}/k_{sol} is about one-half for a material at fusion. Therefore, we assume

$$k_{liq} = 1 \times 10^5 \text{ erg/cm sec } ^\circ\text{K}$$

We find: $K_1 = 200^\circ$ K, $K_2 = 257^\circ$ K, $\beta_1/\rho_b u_b = 44.75$ cm sec/gm, and $\beta_2/\beta_1 = 2.46$. For the Příbram meteor, the depth of the molten layer and the depth for 1 percent temperature rise are shown in figure 8. The interior temperature distribution at 55 km altitude is shown in figure 9. The calculations show that the depths of significant heating in the meteoric body are very small.

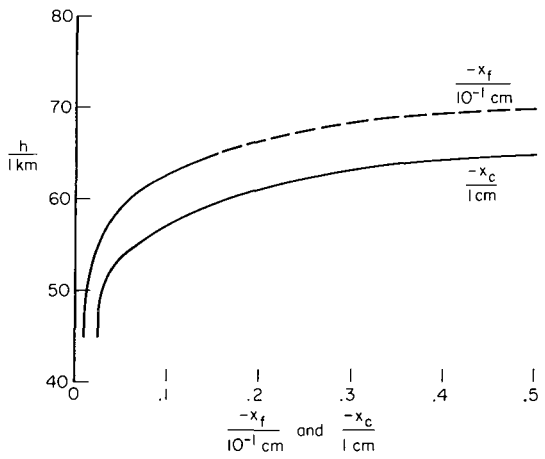

Figure 8.- Depth of molten layer ($-x_f$) and depth of 1-percent temperature rise from cold state ($-x_c$) ($r_b^* = 20$ cm, s = 2).

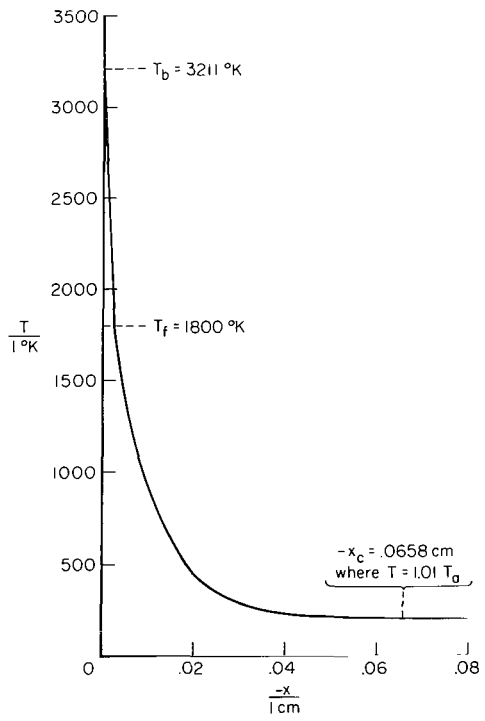

Figure 9.- Representative interior temperature distribution (55 km altitude, $r_b^* = 20$ cm, s = 2).

APPENDIX D

CALCULATION PROCEDURE

The flight parameters are calculated as follows:

1. Specify as input:

   Tables of altitude and flight data: $g \sin \theta$ and h vs. $\overline{\rho}$ (table I); h vs. V and dV/dt (table V(c) for $r_b^* = 20$ cm)

   Constants: ρ_{SL} (eq. (2)); M_b (eq. (38)); s (eq. (21d)); ρ_m, c_{sol}, c_{liq}, T_a, T_f, L_f, L_v, R, and γ (table II)

2. Specify altitude h

3. Compute shock density ratio $\tilde{k} = \rho_\infty/\rho_2$ (eq. (3))

4. Compute $\overline{D}$ (function of radius and standoff distances; see eq. (4)) by using trial values for $\overline{D}$ and iterating until $\lambda(\tilde{k}, \overline{D}) = 0$ (eq. (6))

5. Compute:

$$\rho_\infty = \rho_{SL} \cdot \overline{\rho} = \text{ambient density at altitude h (eq. (1))}$$

$$p_o = \rho_\infty V^2 \approx \text{stagnation pressure (eq. (15))}$$

$$I = I(\overline{\rho}, V) = \text{outer shock-layer radiation rate per unit volume behind normal shock (eq. (7))}$$

$$\left(\frac{C_{H_r}}{r_b}\right)_{ff} = \frac{I(\overline{D} - 1)}{\rho_\infty V^3} \quad \text{(eq. (10))}$$

$$\frac{C_{D_{eff}}}{r_b} = \frac{8}{3} \frac{\rho_m(-dV/dt + g \sin \theta)}{\rho_\infty V^2} \quad \text{(eq. (13))}$$

$$Z = \frac{\frac{1}{s} V \left(\frac{C_{H_r}}{r_b}\right)_{ff}}{\frac{C_{D_{eff}}}{r_b}} \quad \text{(eq. (14'))}$$

6. Determine M_e and other quantities by using trial values of M_e and iterating until $\sigma \equiv Z - Z' = 0$, where the following quantities must be computed for each trial value of M_e:

$$p_e = p_e(p_o, M_e, \gamma) \text{ (eq. (16))}$$

$$\alpha = \alpha(M_e, M_b, \gamma) \text{ (eq. (40))}$$

$$\rho_e/\rho_b = 1/\alpha \text{ (eq. (39))}$$

$$T_e/T_b = \text{function of } \gamma, M_b, \alpha \text{ (eq. (41))}$$

$$p_e/p_b = \alpha M_b^2/M_e^2 \text{ (eq. (42))}$$

$$Ch_c = \text{function of } \alpha, \gamma, M_e, M_b \text{ (eq. (43))}$$

$$p_b = \frac{p_e}{p_e/p_b}$$

$$T_b = T_b(p_b) \text{ (eq. (36b))}$$

$$\zeta_{ab} = c_{sol}(T_f - T_a) + L_f + c_{liq}(T_b - T_f) + L_v \text{ (eq. (25))}$$

$$Z' = Z'(\gamma, R, T_b, M_b, \zeta_{ab}, Ch_c) \text{ (eq. (35))}$$

$$\sigma = Z - Z'$$

7. Then compute:

$$\rho_b = p_b/RT_b \text{ (eq. (34))}$$

$$u_b = M_b\sqrt{\gamma RT_b}$$

$$(C_{H_r})_{ff} = \frac{2\rho_b u_b^3}{\rho_\infty V^3}\left(\frac{\zeta_{ab}}{u_b^2} + \frac{1}{2}\right) \text{ (eq. (30))}$$

$$C_{H_r} = \frac{1}{s}(C_{H_r})_{ff}$$

$$r_b = \frac{(C_{H_r})_{ff}}{(C_{H_r}/r_b)_{ff}}$$

$$C_{D_{eff}} = \left(\frac{C_{D_{eff}}}{r_b}\right) r_b$$

$$(C_{H_c})_{ff} = C_{h_c}\frac{\rho_b u_b^3}{\rho_\infty V^3} \text{ (eq. (31))}$$

$$C_{H_c} = \frac{1}{s} (C_{H_c})_{ff} \quad \text{(eq. (50))}$$

$$C_{D_p} = \frac{p_b}{\frac{s}{2} \rho_\infty V^2} \quad \text{(eq. (47))}$$

$$C_{D_{vc}} = \frac{V(C_{H_c})_{ff}}{su_b} \quad \text{(eq. (48))}$$

$$C_{D_t} = C_{D_{eff}} - C_{D_p} - C_{D_{vc}} \quad \text{(eq. (49))}$$

APPENDIX E

ESTIMATION OF THE VAPOR-ABLATION REYNOLDS NUMBER

The validity of the equations for the boundary shock wave (ref. 1) depends on the vapor-ablation Reynolds number

$$Re_b \equiv \frac{\rho_b u_b d_i}{\tilde{\mu}_b} \tag{E1}$$

being large ($\gg 1$). The quantities ρ_b and u_b are evaluated from calculations presented in the text. To obtain a rough estimation of Re_b, in order to determine rough limits on the applicability of the theory, one must estimate d_i and $\tilde{\mu}_b$.

The shear viscosity, μ, to which $\tilde{\mu}$ is related by

$$\tilde{\mu} = \frac{4}{3}\mu + \frac{1}{3}\kappa \tag{E2}$$

can be estimated using approximate equations from kinetic theory (e.g., see Vincenti and Kruger, ref. 7). Let $\mathcal{m}$ be the molecular weight of the vapor and consider the vapor to be composed of fictitious identical molecules of diameter d. Let ρ_l be the mass density per unit volume of the liquid state of the vapor whose molecular weight is $\mathcal{m}$. Then, denoting Avogadro's number by $\mathcal{L}$, where

$$\mathcal{L} = 6.023 \times 10^{23} \frac{\text{molecules}}{\text{mole}}$$

we may write for the approximate volume occupied by each molecule in the liquid state

$$d^3 = \frac{\mathcal{m}}{\rho_l \mathcal{L}} \tag{E3}$$

The coefficient of shear viscosity (see ref. 7) may be approximated by

$$\mu = \frac{1}{2\pi\sqrt{2}} \frac{\mathcal{m}}{\mathcal{L}} \frac{\bar{c}}{d^2} \tag{E4}$$

where

$$\bar{c} \approx \sqrt{3RT} \tag{E5}$$

Substitution of equations (E3) and (E5) into (E4) gives the approximate relation

$$\mu = \frac{\sqrt{3RT}}{2\sqrt{2}\,\pi}\left(\frac{\mathcal{m}}{\mathcal{L}}\right)\left(\frac{\rho_l \mathcal{L}}{\mathcal{m}}\right)^{2/3} \tag{E6}$$

Now if one assumes

$$\rho_l \approx \rho_m \tag{E7}$$

and takes values for $R, \mathcal{m}$, and ρ_m from table II, one obtains

$$\frac{\mu}{1\ \text{gm cm}^{-1}\ \text{sec}^{-1}} = 0.253\times10^{-4}\left(\frac{T}{1^{\circ}\ \text{K}}\right)^{1/2} \tag{E8}$$

For convenience, one may assume the bulk viscosity κ to be zero, so that (from eq. (E2))

$$\tilde{\mu} = \frac{4}{3}\mu \tag{E9}$$

Then, with the result from equation (38) that

$$u_b = 0.333\sqrt{\gamma RT_b} \tag{E10}$$

equation (E1) with (E8) and (E9) becomes

$$Re_b \equiv \frac{\rho_b u_b d_i}{\tilde{\mu}_b} = \frac{10^7}{0.498}\left(\frac{\rho_b}{1\ \text{gm cm}^{-3}}\right)\left(\frac{r_b}{1\ \text{cm}}\right)\left(\frac{d_i}{r_b}\right) \tag{E11}$$

The estimation of d_i/r_b lies outside the scope of this report. It has been computed from an approximate relationship for which the derivation is rather involved. (The flow field around a sphere with large mass transfer was analyzed.) It will simply be noted here that, corresponding to the calculations for the Příbram meteor (with $r_b^* = 20$ cm and $s = 2$), the following approximate values for d_i/r_b and the resulting Reynolds numbers, Re_b, were found:

$\frac{h}{1\ \text{km}}$	$\frac{d_i}{r_b}$	Re_b
75	0.00507	0.204×10
70	.00939	$.138\times10^2$
65	.01629	$.767\times10^2$
60	.02661	$.354\times10^3$
55	.03928	$.120\times10^4$
50	.05039	$.268\times10^4$
45	.03407	$.857\times10^3$

With little extra effort one can also estimate the thermal conductivity in the vapor:

$$k = \frac{\tilde{\mu} c_p}{\tilde{Pr}} \approx \frac{4}{3} \mu c_p \approx \frac{4}{3} \mu \left(\frac{7}{2} R \right)$$

$$= \frac{14}{3} \mu R \qquad \text{(E12)}$$

With equation (E8) and the value of R from table II, equation (E12) gives

$$\frac{k}{1 \text{ gm cm sec}^{-3} (^{\circ}K)^{-1}} = 196 \left(\frac{T}{1^{\circ} K} \right)^{1/2} \qquad \text{(E13)}$$

REFERENCES

1. Martin, E. Dale: Possible Occurrence of Boundary Shock Waves. NASA TN D-3195, 1966.

2. Allen, H. Julian: On the Motion and Ablation of Meteoric Bodies. Aeronautics and Astronautics, N. J. Hoff and W. G. Vincenti, eds., Pergamon Press, New York, 1960, pp. 378-416.

3. Allen, H. Julian; and James, Nataline A.: Prospects for Obtaining Aerodynamic Heating Results From Analysis of Meteor Flight Data. NASA TN D-2069, 1964.

4. Ceplecha, Zd.: Multiple Fall of Příbram Meteorites Photographed. 1. Double-Station Photographs of the Fireball and Their Relations to the Found Meteorites. Bull. Astronomical Institutes of Czechoslovakia, vol. 12, no. 2, 1961, pp. 21-47.

5. Chapman, Sydney; and Cowling, T. G.: The Mathematical Theory of Non-Uniform Gases. Cambridge University Press, 1961.

6. Hirschfelder, Joseph O.; Curtiss, Charles F.; and Bird, R. Byron: Molecular Theory of Gases and Liquids. John Wiley and Sons, New York, 1964.

7. Vincenti, Walter G.; and Kruger, Charles H., Jr.: Introduction to Physical Gas Dynamics. John Wiley and Sons, Inc., 1965.

8. Lighthill, M. J.: Introduction. Real and Ideal Fluids. Laminar Boundary Layers, ch. I, L. Rosenhead, ed., Oxford, Clarendon Press, 1963, pp. 1-45.

9. Liepmann, H. W.; Narasimha, R.; and Chahine, M. T.: Structure of a Plane Shock Layer. Phys. Fluids, vol. 5, no. 11, Nov. 1962, pp. 1313-1324.

10. Martin, E. Dale: Boundary Shock Waves. J. Fluid Mech., vol. 28, pt. 2, May 8, 1967, pp. 337-352.

11. Nininger, H. H.: Out of the Sky; An Introduction to Meteoritics. Dover Pub., New York, 1952.

12. Öpik, Ernst J.: Physics of Meteor Flight in the Atmosphere. Interscience Pub., New York, 1958.

13. Minzner, R. A.; Champion, K. S. W.; and Pond, H. L.: The ARDC Model Atmosphere 1959. Air Force Surveys in Geophysics No. 115 (AFCRC-TR-59-267), Air Force Cambridge Research Center, Aug. 1959.

14. Allen, H. Julian; Seiff, Alvin; and Winovich, Warren: Aerodynamic Heating of Conical Entry Vehicles at Speeds in Excess of Earth Parabolic Speed. NASA TR R-185, 1963.

15. Lighthill, M. J.: Dynamics of a Dissociating Gas. Part I, Equilibrium Flow. J. Fluid Mech., vol. 2, pt. 1, Jan. 1957, pp. 1-32.

16. Liepmann, H. W.; and Roshko, A.: Elements of Gasdynamics. John Wiley and Sons, Inc., 1957.

17. Wick, Bradford H.: Radiative Heating of Vehicles Entering the Earth's Atmosphere. AGARDograph 68, 1964, pp. 607-627.

18. Bragg, Sir William H.: Concerning the Nature of Things. Dover Pub., New York, 1954.

19. Zemansky, Mark W.: Heat and Thermodynamics. Fourth ed., McGraw-Hill Book Co., Inc., 1957.

TABLE I.- TRAJECTORY DATA FOR ONDŘEJOV METEOR PŘÍBRAM AND ALTITUDE-DENSITY FUNCTION FROM REFERENCE 3

$\sin \theta = 0.6853$; $\tilde{f} = g \sin \theta = 671.5$ cm/sec^2	
Altitude, h/l km	Density function, $\bar{\rho}$
90	$0.284, -5 \equiv 0.284 \times 10^{-5}$
85	.634, -5
80	.173, -4
75	.393, -4
70	.817, -4
65	.158, -3
60	.288, -3
55	.499, -3
50	.884, -3
45	.164, -2

TABLE II.- APPROXIMATE VALUES OF PHYSICAL CONSTANTS APPROPRIATE TO A STONE METEOR

Symbol	Property	Value	Unit	Reference
ρ_m	Mass density of meteor	3.5	gm/cm^3	3
c_{sol}	Specific heat in solid	8.95×10^6	erg/gm $^\circ$K	12
c_{liq}	Specific heat in liquid	1.1×10^7	erg/gm $^\circ$K	12
T_a	Typical cold interior temperature	200	$^\circ$K	12
T_f	Fusion temperature	1800	$^\circ$K	12
L_f	Latent heat of fusion	2.65×10^9	erg/gm	12
L_v	Latent heat of vaporization	6.05×10^{10}	erg/gm	12
$\mathcal{M}$	Molecular weight of vapor	50	gm/mole	12
R	Gas constant	1.66×10^6	cm^2/sec^2 $^\circ$K	3
γ	Ratio of specific heats in vapor, c_p/c_v	1.4		1

TABLE III.- METEOR-TRACKING DATA FOR ONDŘEJOV METEOR PŘÍBRAM (Ref. 4, table 7)

t,sec	h/1 km	$V/10^5$ cm sec^{-1}
0	88.594	20.887 ±0.009
.85806[a]	76.289[a]	20.864 ±.010[a]
.85602[a]	76.318[a]	20.860 ±.007[a]
1.73230	63.837	20.838 ±.013
2.49383	52.970	20.773 ±.013
2.69203	50.164	20.717 ±.013
3.06758	44.858	20.459 ±.024

[a]The data at these two points (both at about h = 76 km) were from two different rotating-shutter cameras. The first two points on the table are from one camera, the remaining five points from the other camera.

TABLE IV.- CALCULATIONS IN CONSTRUCTION OF DATA CURVE

$\frac{h}{1 \text{ km}}$	Values of $\left(\frac{dV/dh}{10^{-5} \text{ sec}^{-1}}\right)$ for r_b* equal to					
	10 cm	15 cm	20 cm	25 cm	35 cm	50 cm
90	-35.6	-39.4	-41.3	-42.45	-43.65	-44.7
85	-21.65	-30.08	-34.35	-36.8	-39.7	-41.9
80	22.03	-.958	-12.4	-19.35	-27.2	-33.1
75	109.7	57.5	31.5	15.8	-2.16	-15.5
70	279.0	170.3	116.2	74.0	46.15	18.45
65	584	373	269	205.3	133.2	79.5

TABLE V.- VELOCITY AND ACCELERATION DATA FROM GRAPHICALLY FITTED CURVES

h / 1 km	V / 10^5 cm sec^{-1}	dV/dh / 10^{-5} sec^{-1}	-dV/dt / 10^3 cm sec^{-2}
	(a) r_b^* = 10 cm		
90	20.877	-35.6	-0.510
85	20.878	-21.65	-.310
80	20.8775	22.03	.3155
75	20.874	109.7	1.569
70	20.863	279.0	3.985
65	20.842	584	8.350
60	20.811	743	10.60
55	20.767	1,085	15.43
50	20.688	2,255	31.97
45	20.468	8,330	116.95
	(b) r_b^* = 15 cm		
90	20.860	-39.4	-0.564
85	20.861	-30.08	-.430
80	20.862	-0.958	-.0137
75	20.860	57.5	.8225
70	20.853	170	2.430
65	20.841	373	5.340
60	20.820	527.5	7.530
55	20.783	960	13.670
50	20.710	2,160	30.64
45	20.470	9,800	137.4
	(c) r_b^* = 20 cm		
90	20.859	-41.3	-0.590
85	20.861	-34.35	-.4905
80	20.862	-12.4	-.1773
75	20.862	31.5	.450
70	20.8575	116.2	1.66
65	20.848	269	3.84
60	20.8285	533	7.61
55	20.791	1,023	14.56
50	20.714	2,300	32.63
45	20.485	10,400	145.8
	(d) r_b^* = 25 cm		
90	20.8585	-42.45	-0.606
85	20.861	-36.8	-.526
80	20.862	-19.35	-.2765
75	20.8615	15.8	.226
70	20.860	74.0	1.059
65	20.853	205.3	2.933
60	20.8375	445	6.360
55	20.802	1,021	14.550
50	20.711	2,910	44.100
45	20.465	7,150	100.2

TABLE V.- VELOCITY AND ACCELERATION DATA FROM GRAPHICALLY FITTED CURVES - Concluded

h / 1 km	V / 10^5 cm sec^{-1}	dV/dh / 10^{-5} sec^{-1}	-dV/dt / 10^3 cm sec^{-2}
(e) r_b* = 35 cm			
90	20.854	-43.65	-0.624
85	20.8565	-39.7	-.567
80	20.858	-27.2	-.3885
75	20.8585	-2.16	-.03085
70	20.8575	46.15	.660
65	20.852	133.2	1.903
60	20.837	480	6.855
55	20.800	1080	15.4
50	20.711	2750	39.0
45	20.4795	8340	117.0
(f) r_b* = 50 cm			
90	20.852	-44.7	-0.639
85	20.854	-41.9	-.599
80	20.856	-33.1	-.473
75	20.8575	-15.5	-.2215
70	20.857	18.45	.264
65	20.854	79.5	1.137
60	20.843	373	5.325
55	20.812	934	13.300
50	20.724	2680	38.00
45	20.480	8070	113.4

NASA-Langley, 1968 —— 12 A-2545

"The aeronautical and space activities of the United States shall be conducted so as to contribute . . . to the expansion of human knowledge of phenomena in the atmosphere and space. The Administration shall provide for the widest practicable and appropriate dissemination of information concerning its activities and the results thereof."

—NATIONAL AERONAUTICS AND SPACE ACT OF 1958

NASA SCIENTIFIC AND TECHNICAL PUBLICATIONS

TECHNICAL REPORTS: Scientific and technical information considered important, complete, and a lasting contribution to existing knowledge.

TECHNICAL NOTES: Information less broad in scope but nevertheless of importance as a contribution to existing knowledge.

TECHNICAL MEMORANDUMS: Information receiving limited distribution because of preliminary data, security classification, or other reasons.

CONTRACTOR REPORTS: Scientific and technical information generated under a NASA contract or grant and considered an important contribution to existing knowledge.

TECHNICAL TRANSLATIONS: Information published in a foreign language considered to merit NASA distribution in English.

SPECIAL PUBLICATIONS: Information derived from or of value to NASA activities. Publications include conference proceedings, monographs, data compilations, handbooks, sourcebooks, and special bibliographies.

TECHNOLOGY UTILIZATION PUBLICATIONS: Information on technology used by NASA that may be of particular interest in commercial and other non-aerospace applications. Publications include Tech Briefs, Technology Utilization Reports and Notes, and Technology Surveys.

Details on the availability of these publications may be obtained from:

SCIENTIFIC AND TECHNICAL INFORMATION DIVISION

NATIONAL AERONAUTICS AND SPACE ADMINISTRATION

Washington, D.C. 20546